Title	Pendular-limit representation of energy levels and spectra of symmetric- and asymmetric-top molecules
Author(s)	Kanya, R; Ohshima, Y
Citation	PHYSICAL REVIEW A (2004), 70(1)
Issue Date	2004-07
URL	http://hdl.handle.net/2433/50061
Right	Copyright 2004 American Physical Society
Type	Journal Article
Textversion	publisher

Pendular-limit representation of energy levels and spectra of symmetric- and asymmetric-top molecules

Reika Kanya and Yasuhiro Ohshima*
Department of Chemistry, Graduate School of Science, Kyoto University, Kitashirakawa-Oiwakecho, Sakyo-ku, Kyoto 606-8502, Japan
(Received 17 March 2004; published 8 July 2004)

We report theoretical investigations pertaining to spectroscopy of pendular-state molecules, which are subjected to the large electrostatic interaction between the molecular dipole and a strong external field. After an appropriate coordinate transformation and a power-series expansion with an order parameter λ that represents the degree of pendular condition, the zeroth-order Hamiltonian for the pendular limit has been derived. Motions of asymmetric tops in a high field are well described as two-dimensional anisotropic harmonic oscillations, and pendular-state quantum numbers have been introduced to label the energy levels. By using perturbative treatments, energies up to the λ^0 order are represented analytically with the pendular-state quantum numbers. Symmetry considerations are also accomplished by using the group theory appropriate to dipolar rigid bodies of symmetric and asymmetric tops in a uniform electric field. Energy levels and wave functions are classified into irreducible representations of the groups and selection rules for optical transitions are described. Energy-level correlations between the field-free and pendular conditions are also discussed on the basis of the group theoretical considerations. For symmetric and asymmetric tops, pendular-limit selection rules on the quantum numbers are derived by expanding the transition-dipole operators on λ, and transition strengths are analytically evaluated for all the excitation configurations with each of the transition types. Utilities of the present formulation have been verified by the comparison with exact model calculations based on the matrix diagonalization with a free-rotation basis set.

DOI: 10.1103/PhysRevA.70.013403 PACS number(s): 33.55.Be, 33.20.−t, 33.70.Ca

I. INTRODUCTION

When a dipolar molecule is in an electric field, the rotation of the molecule is disturbed by Stark effects. If the interaction between the electric dipole moment and the field is larger than the molecular rotational energy, the molecular rotation changes to a pendulumlike libration in the interaction potential, and a molecular orientation is confined in a laboratory frame. Since the situation is far different from a free rotating picture, perturbative treatments based on the picture are unsuitable. Such a condition is called as a "pendular state." The first experimental realization of the "pendular orientation" was accomplished by Loesch and Remscheid [1] in 1990, while techniques of applying an electric field to gas-phase molecules have been utilized for a long time to observe Stark effects in spectra. Combining a rotational cooling by a supersonic expansion and a dc electric field of 30 kV/cm, they oriented CH_3I molecules in a laboratory frame and studied a steric effect in reactive collisions of K atoms with the CH_3I molecules. They termed the method as a "brute force technique." Independently, in 1991, Friedrich and Herschbach [2] reported laser-induced fluorescence observations of ICl molecules in fields up to 20 kV/cm and confirmed that lower rotational states were described well as a pendulumlike libration. The name of "pendular state" was introduced by them. Strongly bound pendular states were realized by Block *et al.* [3] in 1992, who measured infrared spectra of a linear HCN trimer in the 30 kV/cm field and reported a drastic evolution of the spectra from that of a field-free condition. Thereafter, pendular states have been applied to many studies for steric effects of reactions [4], controls of molecular orientation [5–11], measurements of electric dipole moments [12–15], determinations of transition-dipole orientations [16,17], superfluid helium droplet spectroscopies [18–23], and so on [24–28].

On the theoretical side, investigations on polar molecules in a strong electric field has been frequently conducted for more than 70 years. Brouwer [29] studied Stark-effect corrections for a linear molecule up to the fourth order of an electric field in 1930. In 1947, Hughes [30] derived a representation for energy levels of linear rotors in an arbitrary electric field using the continued fraction method. For symmetric-top molecules, Schlier [31] reported the corresponding representation in 1955. Although the results of Hughes and Schlier give accurate solutions in an arbitrary field, their complicated higher-order terms seldom provide clear physical pictures of a strong field case. Exact solutions are also provided by numerical calculations, such as diagonalization of a Hamiltonian matrix constructed by a free-rotor basis set. Because the nature of the pendular states is far different from that of free rotation, the resultant wave functions are represented by highly mixed linear combinations of the free-rotation bases, and gross features of energy levels and spectral pattern for the pendular state can not be expected until the inspection of the numerical outputs. Thus, it is difficult to deduce the physical significance of pendular states from their phenomenological discussions.

In 1957, Peter and Strandberg investigated analytical representations suitable for the pendular-limit condition from a

*Electronic address: ohshima@kuchem.kyoto-u.ac.jp

differential equation of a strong field limit about polar angle θ [32]. They have shown that the motion of a linear rotor in a strong electric field is well described as two-dimensional isotropic harmonic oscillation. Similar treatments were performed by von Meyenn in 1970 [33], and by Bulthuis *et al.* in 1994 [34]. For symmetric tops, the corresponding result was reported by Maergoiz and Troe [35] in 1993 using an extended procedure of the Peter and Strandberg study. In the case of an asymmetric top, on the other hand, it is impossible to reduce the Schrödinger equation into a one-dimensional differential equation about θ. Thus, a simple extension of the above-mentioned method is inadequate. Probably because of this difficulty, there have been no work that derive corresponding pendular-limit representations for asymmetric tops.

Most of the spectroscopic results on molecules in a pendular state [2,3,8–10,12,14,17,36,37] have been analyzed in terms of numerical simulations for individual spectra. In particular, several groups have discussed selection rules associated with the pendular-state spectroscopy. For linear molecules, Rost *et al.* [36] derived the selection rules in terms of a quantum number of pendular vibration from their results of numerical calculations. Moore *et al.* [37] inspected the results of their calculations on a near-prolate asymmetric top and introduced a concept of a "pendular group number," denoted by n, in order to classify eigenstates. They succeeded in finding a selection rule about n for several types of excitation configurations. However, it seems difficult to extend these selection rules applicable to generalized conditions because they have been discovered from the phenomenological considerations on the results of their simulations. For further development of spectroscopy in a strong field, a firm theoretical ground should be provided to the derivation of selection rules and the calculation of line strengths.

Symmetry consideration with group theory is so beneficial for classification of energy levels and derivation of selection rules for interactions and optical transitions. For a molecule in an electric field, ordinary treatments using rotation groups do not hold because of spatial anisotropy. In 1975, Watson derived symmetry groups for rovibronic levels of a molecule in a uniform electric or magnetic field [38]. He developed the theory in terms of molecular symmetry groups, whose symmetry operations are constructed by an inversion through the center of mass and permutations of identical nuclei. Though his basic idea is universal, the original results cannot be utilized for a rigid body of symmetric or asymmetric tops, where no nucleus is defined. Thus, some modification should be introduced to classify pendular-state energy levels of symmetric- and asymmetric-top molecules.

The present paper aims to establish foundations for describing characteristics of molecules in the pendular state and spectroscopy related to them, which have not been fully explored as mentioned above by the preceding experimental and theoretical studies. The organization of the paper is as follows. A comprehensive consideration on limiting behaviors of asymmetric-top molecules in a strong electric field is described in Sec. II. We first derive wave functions and corresponding eigenvalues in the high-field limit by adopting an appropriate coordinate transformation. Pendular-state quantum numbers for asymmetric tops are introduced for the first time, and the implication of the results is discussed. Then, a symmetry group suitable to a rigid asymmetric top in a uniform electric field is constructed to classify the pendular-state energy levels. In terms of the presently developed pendular-limit formalism and symmetry group consideration, optical selection rules pertaining to the pendular-state quantum numbers are discussed, and approximate representations of transition dipole matrix elements are derived for all the excitation configurations with each of the transition types. In Sec. III, the similar considerations are described for symmetric-top molecules. In Sec. IV, in order to verify the above-mentioned results and their utilities, the derived analytical formulations for energy levels and line strengths are assessed by the comparison with numerical results from the direct diagonalization of the Hamiltonian matrix. This is followed by a brief conclusion in Sec. V.

II. ASYMMETRIC TOP IN PENDULAR STATES

In this section, we mainly describe the pendular state of a specific asymmetric-top molecule whose electric dipole moment, μ, is parallel to one of the principal axes. In this paper, we call such an asymmetric top as a specified asymmetric top. General asymmetric tops will be briefly discussed in Sec. II G.

A. Energy levels and wave functions

First, we define an axis system. We choose a (right-handed) space-fixed axis whose Z component directs to the external electric field vector, $\boldsymbol{\epsilon}$. A (right-handed) molecular-fixed axes are defined as follows: the direction of z is parallel to μ, and the x,y axes are identical to the other principal axes. For example, molecular-fixed x and y axes corresponds to the a and b principal axes, respectively, if $\mu \| c$. In this axis system, Hamiltonian of a polar asymmetric top in a uniform electric field is

$$\hat{H} = \mathcal{B}_x \hat{j}_x^2 + \mathcal{B}_y \hat{j}_y^2 + \mathcal{B}_z \hat{j}_z^2 - \mu\epsilon \cos\theta, \tag{1}$$

where $\mathcal{B}_x$, $\mathcal{B}_y$, and $\mathcal{B}_z$ are the rotational constants around the x, y, and z axes, respectively. $\hat{j}_x$, $\hat{j}_y$, and $\hat{j}_z$ are the molecular-fixed components of the total angular momentum, j,

$$\hat{j}_x = -i \cos\chi \left(\cot\theta \frac{\partial}{\partial\chi} - \frac{1}{\sin\theta} \frac{\partial}{\partial\phi} \right) - i \sin\chi \frac{\partial}{\partial\theta}, \tag{2a}$$

$$\hat{j}_y = i \sin\chi \left(\cot\theta \frac{\partial}{\partial\chi} - \frac{1}{\sin\theta} \frac{\partial}{\partial\phi} \right) - i \cos\chi \frac{\partial}{\partial\theta}, \tag{2b}$$

$$\hat{j}_z = -i \frac{\partial}{\partial\phi}, \tag{2c}$$

where ϕ, θ, χ are Euler angles. The reduction of Eq. (1) with the energy unit of $(\mathcal{B}_x+\mathcal{B}_y)/2$ yields

$$\hat{H} = \sigma_x \hat{j}_x^2 + \sigma_y \hat{j}_y^2 + \sigma_z \hat{j}_z^2 - \frac{2}{\lambda^2}\cos\theta, \tag{3}$$

where σ_g $(g=x,y,z)$ and λ are

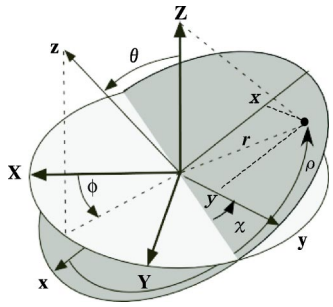

FIG. 1. Variable definitions.

$$\sigma_g = \frac{2\mathcal{B}_g}{\mathcal{B}_x + \mathcal{B}_y}, \tag{4a}$$

$$\lambda = \sqrt{\frac{\mathcal{B}_x + \mathcal{B}_y}{\mu\epsilon}}, \tag{4b}$$

σ_g is a reduced rotational constant about the g axis. σ_x and σ_y ranges from 0 to 2, while $\sigma_z > 0$. λ is the most important parameter in this paper, which represents the degree of pendular condition. As $\mu\epsilon$ becomes larger than the rotational constants, λ approaches to zero. We introduce an index for asymmetry, σ, as

$$\sigma = (\sigma_x - \sigma_y)/2, \tag{5}$$

which ranges from -1 to 1. In the symmetric-top case, $\sigma = 0$. σ_x and σ_y are represented by the single parameter σ as follows: $\sigma_x = 1+\sigma$, $\sigma_y = 1-\sigma$.

Next, we transform the variables, i.e., the Euler angles, into new variables that are suitable to describe the pendular vibration. It is important to choose properly a variable transformation for a clear description of pendular states of an asymmetric top. The nature of pendular vibrations around the x axis is not the same as that around the y axis because of the difference between $\mathcal{B}_x$ and $\mathcal{B}_y$ of asymmetric-top molecules. Thus, new variables should determine the direction of displacement in the molecular-fixed axis system. Here, we adopt the following transformation:

$$\psi = \phi + \chi, \tag{6a}$$

$$x = r\cos\rho, \tag{6b}$$

$$y = r\sin\rho, \tag{6c}$$

where

$$r = \frac{2}{\sqrt{\lambda}}\tan\frac{\theta}{2}, \tag{7a}$$

$$\rho = \pi - \chi. \tag{7b}$$

As shown in Fig. 1, ρ determines the direction of ϵ measured from the x axis, and r stands for the reduced magnitude of the ϵ displacement, which ranges from zero to infinity. Thus, the orientation of μ in the space-fixed axis is interpreted as the position of ϵ in the molecular-fixed xy plane.

After the above-mentioned variable transformation of $(\phi,\theta,\chi)\rightarrow(\psi,x,y)$,

$$\frac{\partial}{\partial\phi} = \frac{\partial}{\partial\psi}, \tag{8a}$$

$$\frac{\partial}{\partial\theta} = \frac{1+\frac{x^2+y^2}{4}\lambda}{\sqrt{\lambda(x^2+y^2)}}\left(x\frac{\partial}{\partial x} + y\frac{\partial}{\partial y}\right), \tag{8b}$$

$$\frac{\partial}{\partial\chi} = \frac{\partial}{\partial\psi} + y\frac{\partial}{\partial x} - x\frac{\partial}{\partial y} \tag{8c}$$

are obtained. The trigonometric functions of θ appearing in Eqs. (2) are also transformed, and expanded into the power series of λ. After the procedure, transformed Hamiltonian of Eq. (3) is arranged according to the order of λ. The leading term is in the order of λ^{-2} as

$$\hat{H}_{\lambda^{-2}} = -\frac{2}{\lambda^2}. \tag{9}$$

This term represents the zero-point shift, which is constant and independent of the rotational constants. This result is reasonable from the fact that the interaction potential is expressed as $-2\cos\theta/\lambda^2$ in Eq. (3), which has a limiting value of $\approx -2/\lambda^2$ when the whole molecules are oriented along the electric field.

The terms of the λ^{-1} order are described as

$$\hat{H}_{\lambda^{-1}} = \lambda^{-1}\hat{h}_0^a, \tag{10}$$

where

$$\hat{h}_0^a = -\sigma_y\frac{\partial^2}{\partial x^2} + x^2 - \sigma_x\frac{\partial^2}{\partial y^2} + y^2. \tag{11}$$

Equation (11) represents a two-dimensional anisotropic harmonic oscillator, which is independent of ψ. We consider $\hat{H}_{\lambda^{-1}}$ as the zeroth-order Hamiltonian.

The form of Eq. (11) enables us to treat the three coordinates (ψ,x,y), separately. An ordinary procedure for a problem of harmonic oscillators yields

$$E^{(0)}_{v_x,v_y,m} = 2\sqrt{\sigma_y}(v_x + \tfrac{1}{2}) + 2\sqrt{\sigma_x}(v_y + \tfrac{1}{2}) \tag{12}$$

for the eigenvalue of $\hat{h}_0^a$. The corresponding zeroth-order wave function is represented as

$$|v_x,v_y,m\rangle = N_{v_x,v_y}H_{v_x}(\sigma_y^{-1/4}x)H_{v_y}(\sigma_x^{-1/4}y) \times\exp\left[-\frac{x^2}{2\sigma_y^{1/2}} - \frac{y^2}{2\sigma_x^{1/2}}\right]e^{im\psi}, \tag{13}$$

where $H_n(\xi)$ stands for a Hermite polynomial. The relation of

$$\hat{J}_Z = -i\frac{\partial}{\partial\phi} = -i\frac{\partial}{\partial\psi} \tag{14}$$

shows that the quantum number m in Eq. (13) is identical to the quantum number for rotation around the Z axis. v_x and v_y in Eqs. (12) and (13) express quantum numbers for harmonic

vibrations along the x and y axes, respectively. The constant N_{v_x,v_y} in Eq. (13) is defined as

$$N_{v_x,v_y} = (2^{v_x+v_y+1}\lambda\pi^2 v_x!\, v_y!\, \sigma_x^{1/4}\sigma_y^{1/4})^{-1/2}. \tag{15}$$

Since $\hat{h}_0^a$ is independent of ψ, the zeroth-order wave function would be an arbitrary function of ψ. We choose $e^{im\psi}$ on the grounds that it is an irreducible representation of a group appropriate to an asymmetric top in an external uniform field, as will be shown in Sec. II B.

It should be noted that the basis set of $|v_x,v_y,m\rangle$ is not orthonormal. Since a volume element of the integral of this case is represented as

$$d\mathbf{v} = \sin\,\theta\, d\phi\, d\theta\, d\chi = \lambda\left(1+\frac{x^2+y^2}{4}\lambda\right)^{-2} d\psi\, dx\, dy, \tag{16}$$

the orthogonal relation of Hermite polynomials does not lead to an orthogonality of $|v_x,v_y,m\rangle$. Then, $\hat{h}_0^a$ is proved to be a non-Hermite operator as follows:

$$\int |v_x',v_y',m'\rangle^* \hat{h}_0^a |v_x'',v_y'',m''\rangle d\mathbf{v} - \left[\int |v_x'',v_y'',m''\rangle \hat{h}_0^a |v_x',v_y',m'\rangle^*\, d\mathbf{v}\right]^* = (E^{(0)}_{v_x'',v_y'',m''} - E^{(0)}_{v_x',v_y',m'}) \int |v_x',v_y',m'\rangle^* |v_x'',v_y'',m''\rangle d\mathbf{v} \neq 0. \tag{17}$$

Similarly, x, y, $\hat{p}_x$, and $\hat{p}_y$ are found to be non-Hermite operators, while $e^{\pm i\psi}$ are Hermite operators. The volume element, $d\mathbf{v}$, can be expanded in λ as

$$\begin{aligned} d\mathbf{v} &= \left(1-\frac{x^2+y^2}{2}\lambda+\frac{3(x^2+y^2)^2}{16}\lambda^2-\cdots\right)\lambda\, d\psi\, dx\, dy \\ &= \left(1-\frac{x^2+y^2}{2}\lambda+\frac{3(x^2+y^2)^2}{16}\lambda^2-\cdots\right) d\mathbf{v}', \end{aligned} \tag{18}$$

where $d\mathbf{v}'$ is the volume element in the strong-field limit, namely $\lambda\to 0$. Therefore, in the strong-field limit, $|v_x,v_y,m\rangle$ can be regarded as orthonormal and we can treat $\hat{h}_0^a$, x, y, $\hat{p}_x$, and $\hat{p}_y$ as Hermite operators, where

$$\hat{p}_x = -i\frac{\partial}{\partial x}, \tag{19a}$$

$$\hat{p}_y = -i\frac{\partial}{\partial y}. \tag{19b}$$

Matrix elements of these operators are derived analytically in the case by using the recursion formula of Hermite polynomials. The nonzero matrix elements of x, y, $\hat{p}_x$, and $\hat{p}_y$ are

$$\langle v_x\pm 1,v_y,m|x|v_x,v_y,m\rangle = \left[\frac{\sigma_y^{1/2}}{2}\left(v_x+\frac{1}{2}\pm\frac{1}{2}\right)\right]^{1/2}, \tag{20a}$$

$$\langle v_x,v_y\pm 1,m|y|v_x,v_y,m\rangle = \left[\frac{\sigma_x^{1/2}}{2}\left(v_y+\frac{1}{2}\pm\frac{1}{2}\right)\right]^{1/2}, \tag{20b}$$

$$\langle v_x\pm 1,v_y,m|\hat{p}_x|v_x,v_y,m\rangle = \pm i\left[\frac{1}{2\sigma_y^{1/2}}\left(v_x+\frac{1}{2}\pm\frac{1}{2}\right)\right]^{1/2}, \tag{20c}$$

$$\langle v_x,v_y\pm 1,m|\hat{p}_y|v_x,v_y,m\rangle = \pm i\left[\frac{1}{2\sigma_x^{1/2}}\left(v_y+\frac{1}{2}\pm\frac{1}{2}\right)\right]^{1/2}. \tag{20d}$$

The nonzero matrix elements of $e^{\pm i\psi}$ are

$$\langle v_x,v_y,m\pm 1|e^{\pm i\psi}|v_x,v_y,m\rangle = 1. \tag{21}$$

Hereafter, the strict integral of an operator $\hat{A}$ is expressed as $\int |v_x',v_y',m'\rangle^* \hat{A} |v_x'',v_y'',m''\rangle d\mathbf{v}$, where $d\mathbf{v}$ of Eq. (16) is used as the volume element. On the other hand, $\langle v_x',v_y',m'|\hat{A}|v_x'',v_y'',m''\rangle$ denotes an integral in the strong-field limit, where $d\mathbf{v}'$ is used. The relation of

$$\begin{aligned} &\int |v_x',v_y',m'\rangle^* \hat{A} |v_x'',v_y'',m''\rangle d\mathbf{v} \\ &= \langle v_x',v_y',m'|\left(1+\frac{x^2+y^2}{4}\lambda\right)^{-2}\hat{A}|v_x'',v_y'',m''\rangle \end{aligned} \tag{22}$$

holds between the two expressions.

The λ^0 term of the expanded Hamiltonian is

$$\hat{H}_{\lambda^0} = (\hat{f}_1+\tfrac{1}{2}\hat{f}_2) + \sigma_z(\hat{j}_Z-\hat{l})^2 - \tfrac{1}{4}(x^2+y^2)^2, \tag{23}$$

where

$$\hat{l} = x\hat{p}_y - y\hat{p}_x, \tag{24a}$$

$$\hat{f}_1 = (\sigma_x x\hat{p}_y - \sigma_y y\hat{p}_x)\hat{j}_Z, \tag{24b}$$

$$\hat{f}_2 = -(\sigma_x x\hat{p}_y - \sigma_y y\hat{p}_x)\hat{l} + (\sigma_y x\hat{p}_x + \sigma_x y\hat{p}_y)\hat{u}, \tag{24c}$$

$$\hat{u} = x\hat{p}_x + y\hat{p}_y. \tag{24d}$$

Due to the nonorthonormality of the zeroth-order wave functions, careful treatments are necessary to utilize a perturbation theory. In the present case, matrix elements can be ex-

TABLE I. Euler angle transformations under symmetry operations of K(spatial) and D_2.

Operation	ϕ transformation	θ transformation	χ transformation
E	$\phi\rightarrow\phi$	$\theta\rightarrow\theta$	$\chi\rightarrow\chi$
$C^Z(\delta)$	$\phi\rightarrow\phi+\delta$	$\theta\rightarrow\theta$	$\chi\rightarrow\chi$
$C_\alpha^{\perp Z}(\pi)$	$\phi\rightarrow 2\alpha-\phi$	$\theta\rightarrow\pi-\theta$	$\chi\rightarrow\chi+\pi$
$C_z(\pi)$	$\phi\rightarrow\phi$	$\theta\rightarrow\theta$	$\chi\rightarrow\chi+\pi$
$C_x(\pi)$	$\phi\rightarrow\phi+\pi$	$\theta\rightarrow\pi-\theta$	$\chi\rightarrow-\chi$
$C_y(\pi)$	$\phi\rightarrow\phi+\pi$	$\theta\rightarrow\pi-\theta$	$\chi\rightarrow\pi-\chi$

panded into the power series of λ, see Eqs. (18) and (22). The perturbation theory in this situation is discussed briefly in Appendix A. The first-order perturbation treatment yields the correction to the energy as

$$E_{v_x,v_y,m}(\lambda^0) = -\frac{\sigma_y}{8}\left(v_x+\frac{1}{2}\right)^2-\frac{\sigma_x}{8}\left(v_y+\frac{1}{2}\right)^2 + \frac{1}{2}\left(\frac{4\sigma_z}{\sigma_x^{1/2}\sigma_y^{1/2}}-3\sigma_x^{1/2}\sigma_y^{1/2}\right)\left(v_x+\frac{1}{2}\right)\left(v_y+\frac{1}{2}\right) + \sigma_z m^2-\frac{\sigma_z}{2}-\frac{1}{16}. \quad (25)$$

The effect of the Z-axis rotation appears in Eq. (25) as $\sigma_z m^2$. Since $E_{v_x,v_y,m}(\lambda^0)$ is independent of λ, $E_{v_x,v_y,m}(\lambda^0)$ does not approach to zero even in a strong-field limit. Therefore, the energy-level representation in a strong-field limit is expressed up to the λ^0 order as

$$E_{v_x,v_y,m}^{\lambda\rightarrow 0} = -\frac{2}{\lambda^2}+\frac{2\sigma_y^{1/2}}{\lambda}\left(v_x+\frac{1}{2}\right)+\frac{2\sigma_x^{1/2}}{\lambda}\left(v_y+\frac{1}{2}\right) + E_{v_x,v_y,m}(\lambda^0). \quad (26)$$

B. Symmetry considerations

In this section, symmetry considerations for pendular states are described. In the case of free rotation of an asymmetric top, the spatial three-dimensional pure rotation group, denoted K(spatial), and molecular rotation group of D_2 can be used. In a uniform electric field, however, it is impossible to use either K(spatial) or D_2 because of the interaction between μ and ϵ. Therefore, some suitable group should be constructed.

First, we seek symmetry operations for the full Hamiltonian of Eq. (1). Apparently, the identity operator, E, is a symmetry operation. Among the symmetry operations in K(spatial), arbitrary rotations around the Z axis, denoted $C^Z(\delta)$ where δ is an arbitrary angle, are still symmetry operations because of the isotropy around the Z axis. Although any rotation around other spatial axes is not a symmetry operation, we consider π rotations about arbitrary axes in the XY plane, and express as $C_\alpha^{\perp Z}(\pi)$ where α denotes the angle measured from the X axis to the rotation axis. As for the operations of D_2, π rotation around the z axis, $C_z(\pi)$, is still a symmetry operation while π rotations around the x and y axes, denoted $C_x(\pi)$ and $C_y(\pi)$, respectively, are not. From the Euler angle transformations depicted in Table I, $C_\alpha^{\perp Z}(\pi)C_x(\pi)$ and $C_\alpha^{\perp Z}(\pi)C_y(\pi)$ become symmetry operations. As a result, it can be derived that the following symmetry operations form a group:

$$\{E, C_z(\pi), C^Z(\delta), C^Z(\delta)C_z(\pi), C_\alpha^{\perp Z}(\pi)C_x(\pi), C_\alpha^{\perp Z}(\pi)C_y(\pi)\}, \quad (27)$$

where δ and α are arbitrary angles.

According to the relations among the operators, e.g.,

$$[C_\alpha^{\perp Z}(\pi)C_x(\pi)]^{-1}C^Z(\delta)[C_\alpha^{\perp Z}(\pi)C_x(\pi)]=C^Z(-\delta) \quad (28)$$

the symmetry operators can be divided into classes. The character table of this group is shown in Table II. Transformation of ϕ, χ, x, and y under the symmetry operations is also indicated in the table. In addition, symmetries of x, y, z,

TABLE II. Character table for an asymmetric top in a uniform external field.

	E	$C_z(\pi)$	$C^Z(\delta)$ $C^Z(-\delta)$	$C^Z(\delta)C_z(\pi)$ $C^Z(-\delta)C_z(\pi)$	$\infty C_x(\pi)C_\alpha^{\perp Z}(\pi)$	$\infty C_y(\pi)C_\alpha^{\perp Z}(\pi)$	
$\phi\rightarrow$	ϕ	ϕ	$\phi\pm\delta$	$\phi\pm\delta$	$\pi-\phi+2\alpha$	$\pi-\phi+2\alpha$	
$\chi\rightarrow$	χ	$\chi+\pi$	χ	$\chi+\pi$	$\pi-\chi$	$-\chi$	
$\psi\rightarrow$	ψ	$\psi+\pi$	$\psi\pm\delta$	$\psi+\pi\pm\delta$	$-\psi+2\alpha$	$\pi-\psi+2\alpha$	
$x\rightarrow$	x	$-x$	x	$-x$	$-x$	x	
$y\rightarrow$	y	$-y$	y	$-y$	y	$-y$	
$(0^+,A)$	1	1	1	1	1	1	z
$(0^-,A)$	1	1	1	1	−1	−1	$\hat{j}_Z$, $\hat{j}_z$
(M,A)[a]	2	2	$2\cos M\delta$	$2\cos M\delta$	0	0	
$(0^+,B)$	1	−1	1	−1	1	−1	y, $\hat{j}_x$
$(0^-,B)$	1	−1	1	−1	−1	1	x, $\hat{j}_y$
(M,B)[a]	2	−2	$2\cos M\delta$	$-2\cos M\delta$	0	0	

[a] $M=1,2,3,\ldots$.

TABLE III. Symmetry of pendular-state wave function, $|v_x, v_y, m\rangle$.

m	(v_x, v_y)	Symmetry
0	(even, even)	$(0^+, A)$
0	(odd, odd)	$(0^-, A)$
0	(even, odd)	$(0^+, B)$
0	(odd, even)	$(0^-, B)$
even[a]	(even, even) or (odd, odd)	$(\|m\|, A)$
even[a]	(even, odd) or (odd, even)	$(\|m\|, B)$
odd	(even, even) or (odd, odd)	$(\|m\|, B)$
odd	(even, odd) or (odd, even)	$(\|m\|, A)$

[a] $m \neq 0$.

$\hat{j}_x$, $\hat{j}_y$, $\hat{j}_z$, and $\hat{j}_Z$ are shown at the last column. Symmetry of other operators are as follows: $(0^-, B)$ for $\hat{R}_x^{\pm}$, $(0^+, B)$ for $\hat{R}_y^{\pm}$, and $(1, B)$ for $\hat{j}_Z^{\pm}$, where $\hat{R}_x^{\pm}$, $\hat{R}_y^{\pm}$, and $\hat{j}_Z^{\pm}$ are the ladder operator of the vibration along the x, y axes and the rotation around the Z axis, respectively. They are represented as

$$\hat{R}_x^{\pm} = \sigma_y^{1/2} \hat{p}_x \pm i x, \tag{29a}$$

$$\hat{R}_y^{\pm} = \sigma_x^{1/2} \hat{p}_y \pm i y, \tag{29b}$$

$$\hat{j}_Z^{\pm} = e^{\pm i\psi}. \tag{29c}$$

Table II reveals that the zeroth-order wave functions of Eqs. (13) are irreducible representations, and their symmetries are summarized in Table III.

Finally, we discuss symmetry of the basis set of free rotation. If we denote the wave function of a free-rotating symmetric top as $|j, k, m\rangle_f$, where the subscript f is added to avoid confusion, the symmetrized basis set is expressed as follows:

$$\text{(i) } m = 0, k = 0: |j, 0, 0\rangle_f, \tag{30a}$$

$$\text{(ii) } m = 0, k \neq 0: |j, |k|, 0, s\rangle_f = \{|j, |k|, 0\rangle_f + (-1)^s |j, -|k|, 0\rangle_f\}/\sqrt{2}, \tag{30b}$$

$$\text{(iii) } m \neq 0: \begin{pmatrix} |j, k, |m|\rangle_f \\ |j, -k, -|m|\rangle_f \end{pmatrix}, \tag{30c}$$

where $s = 0$ or 1, and symmetry of the basis is summarized in Table IV. From Table IV, the symmetry correlation can be derived between the finite-field case and field-free case, where K (spatial) and D_2 groups are defined. The results are shown in Table V.

C. Higher-order correction terms

In Sec. II A, Hamiltonian of Eq. (3) was expanded into the power series of λ, and only the terms of λ^{-2}, λ^{-1}, and λ^0 are considered. The higher-order terms, denoted $\hat{H}_{\lambda^n}$ for λ^n, are

TABLE IV. Symmetry of the field-free basis.

Configuration	Symmetry
$m=0$, $k=0$	$(0^+, A)$
$m=0$, $k=$even,[a] $s=0$	$(0^+, A)$
$m=0$, $k=$even,[a] $s=1$	$(0^-, A)$
$m=0$, $k=$odd, $s=0$	$(0^+, B)$
$m=0$, $k=$odd, $s=1$	$(0^-, B)$
$m \neq 0$, $k=$even	$(\|m\|, A)$
$m \neq 0$, $k=$odd	$(\|m\|, B)$

[a] $k \neq 0$.

$$\hat{H}_{\lambda^1} = \lambda\left[\tfrac{1}{4}\hat{f}_3 + \tfrac{1}{16}\hat{f}_4 - \tfrac{1}{4}\hat{f}_5 + \tfrac{1}{2}\hat{f}_6 - \tfrac{1}{4}\hat{f}_7 + \tfrac{1}{8}\hat{f}_8 + \tfrac{1}{16}(x^2 + y^2)^3\right], \tag{31a}$$

$$\hat{H}_{\lambda^n} = \lambda^n (-1)^{n+1} \frac{(x^2 + y^2)^{n+2}}{4^{n+1}} \quad (n \geq 2), \tag{31b}$$

where

$$\hat{f}_3 = (\sigma_x x^2 + \sigma_y y^2)\hat{j}_Z^2, \tag{32a}$$

$$\hat{f}_4 = (\sigma_x x^2 + \sigma_y y^2)(\hat{l}^2 + \hat{u}^2), \tag{32b}$$

$$\hat{f}_5 = (\sigma_x x^2 + \sigma_y y^2)\hat{l}\hat{j}_Z, \tag{32c}$$

$$\hat{f}_6 = \sigma x y(\hat{u} - i)\hat{j}_Z, \tag{32d}$$

$$\hat{f}_7 = \sigma x y(\hat{u} - i)\hat{l}, \tag{32e}$$

$$\hat{f}_8 = i\sigma(x^2 - y^2)\hat{u}. \tag{32f}$$

The kinetic contributions are exactly expressed by the expansion up to the λ^1 order. Equation (31b) and the last term of

TABLE V. Symmetry correlation between the field-free and finite-field cases.

Zero field		
K(spatial)	D_2	Finite field
$m=0$, $j=$even	A	$(0^+, A)$
$m=0$, $j=$even	B_z	$(0^-, A)$
$m=0$, $j=$even	B_x	$(0^+, B)$
$m=0$, $j=$even	B_y	$(0^-, B)$
$m=0$, $j=$odd	A	$(0^-, A)$
$m=0$, $j=$odd	B_z	$(0^+, A)$
$m=0$, $j=$odd	B_x	$(0^-, B)$
$m=0$, $j=$odd	B_y	$(0^+, B)$
$m \neq 0$, any j	A	$(\|m\|, A)$
$m \neq 0$, any j	B_z	$(\|m\|, A)$
$m \neq 0$, any j	B_x	$(\|m\|, B)$
$m \neq 0$, any j	B_y	$(\|m\|, B)$

Eq. (31a) come from the anharmonicity of the interaction cosine potential. Since λ is sufficiently small in a strong-field condition, a perturbative treatment is effective to include higher-order Hamiltonians of Eqs. (31).

For larger vibrational quantum numbers, $v_{x,y}$, the perturbative treatment becomes inadequate for reproductions of energy levels. This comes from the state congestion of high energy levels and the ill convergence in the λ expansion of the cosine potential. The dipole-field interaction potential is expanded as

$$-\frac{2}{\lambda^2}\cos\theta = -\frac{2}{\lambda^2}\left(\frac{1-(x^2+y^2)\lambda/4}{1+(x^2+y^2)\lambda/4}\right) = -\frac{2}{\lambda^2}\left(1-\frac{x^2+y^2}{2}\lambda+\frac{(x^2+y^2)^2}{8}\lambda^2 - \cdots + (-1)^k\frac{2(x^2+y^2)^k}{4^k}\lambda^k+\cdots\right). \quad (33)$$

This expansion is appropriate only for $x,y\sim 0$, namely around the minimum of the potential. High $v_{x,y}$ states have substantial probability density even at $\theta\sim\pi$, namely $x,y\sim\pm\infty$, and thus extraordinary higher-order terms are necessary to describe the potential. For such cases, a nonperturbative method with the pendular-limit formalism, which will be described in the next section, is appropriate.

D. Nonperturbative treatments

Here, we describe alternative method for reproductions of energy levels, namely a matrix diagonalization method with the pendular-limit formalism. As discussed in Sec. II A, the pendular basis set $|v_x,v_y,m\rangle$ is not orthonormal. Thus, we should solve a generalized eigenvalue problem to calculate energy levels from a Hamiltonian matrix constructed by the basis set, and this procedure requires complicated matrix operations. Then, we introduce an alternative basis set, i.e., an orthonormal pendular basis set, $|v_x,v_y,m\rangle_{\text{o.n.}}$, as

$$|v_x,v_y,m\rangle_{\text{o.n.}} = \left(1+\frac{x^2+y^2}{4}\lambda\right)|v_x,v_y,m\rangle, \quad (34)$$

where $|v_x,v_y,m\rangle$ is defined in Eq. (13). The $|v_x,v_y,m\rangle_{\text{o.n.}}$ is orthonormal in the integral with the exact volume element of Eq. (16). It should be noted that this basis is not an eigenfunction of the zeroth-order Hamiltonian, while it nearly behaves as an eigenfunction in the pendular limit.

$$\hat{h}_0^a|v_x,v_y,m\rangle_{\text{o.n.}} = E^{(0)}_{v_x,v_y,m}|v_x,v_y,m\rangle_{\text{o.n.}} + \lambda\left(1+\frac{x^2+y^2}{4}\lambda\right)^{-2}\left[\frac{\sigma_y(v_x+1)(v_x+2)}{2}|v_x+2,v_y,m\rangle_{\text{o.n.}} - \frac{\sigma_y v_x(v_x-1)}{2}|v_x-2,v_y,m\rangle_{\text{o.n.}} + \frac{\sigma_x(v_y+1)(v_y+2)}{2}|v_x,v_y+2,m\rangle_{\text{o.n.}} - \frac{\sigma_x v_y(v_y-1)}{2}|v_x,v_y-2,m\rangle_{\text{o.n.}}\right]. \quad (35)$$

Because differentials of $|v_x,v_y,m\rangle_{\text{o.n.}}$ with x,y can be transformed into nondifferential forms using the recursion formula of Hermite polynomials, matrix elements of the full Hamiltonian are evaluated by numerical calculations on Gauss-Hermite quadratures. After a diagonalization of the Hamiltonian matrix, energy levels and wave functions are obtained. In this procedure, as the numbers of the basis functions and the grid points in the quadratures become larger, we have more precise values. Because obtained wave functions are represented by the orthonormal pendular basis set, which is suitable for the pendular limit, this procedure is more appropriate on interpretations of physical nature of pendular states than the matrix diagonalization method with the free-rotation basis set.

E. Selection rules

First, we discuss the selection rules of optical transitions for the full Hamiltonian of Eq. (3). Because of anisotropy of the space, symmetry of the transition dipole operator depends on the direction of $\mathcal{E}$ in the space-fixed frame, where $\mathcal{E}$ stands for an electric vector of an electromagnetic wave. For the case that $\mathcal{E}$ is parallel to the X or Y axis, the transition dipole operator is expressed as μ_X or μ_Y, respectively. When $\mathcal{E}$ is parallel to the Z axis, μ_Z is used. μ_F $(F=X,Y,Z)$ can be expressed in terms of the direction cosine matrix, $\Phi(\phi,\theta,\chi)$, and the molecule-field transition dipole by

$$\mu_F = \sum_{g=x,y,z}\Phi_{Fg}(\phi,\theta,\chi)\mu_g, \quad (36)$$

where μ_x, μ_y, and μ_z denoted the x,y, and z components of the transition dipole, respectively. The transformation property of the direction cosine matrix elements can be derived from Euler angle transformations in Table II. Therefore, the symmetry of each x,y,z component of μ_F can be determined, and is shown in Table VI. Combining Tables III and VI, selection rules in terms of the zeroth-order wave function, Eq. (13), are derived as listed in Table VII.

As shown in Table VI, the pair of μ_X and μ_Y constructs doubly degenerated representations. Thus, it is enough to consider only μ_X for the transition in the $\mathcal{E}\perp\epsilon$ configuration. We express μ_g component of μ_F as μ_{Fg}, where $F=X,Y,Z$ and $g=x,y,z$. Then, $(\phi,\theta,\chi)\rightarrow(\psi,x,y)$ transformation of μ_{Zg} yields

TABLE VI. Symmetries of transition dipoles.

Transition dipole	Transition type	Symmetry
μ_Z	μ_x	$(0^-,B)$
	μ_y	$(0^+,B)$
	μ_z	$(0^+,A)$
$\begin{pmatrix}\mu_X\\ \mu_Y\end{pmatrix}$	μ_x	$(1,B)$
	μ_y	$(1,B)$
	μ_z	$(1,A)$

$$\mu_{Zx} = -\mu_x \sin\theta\cos\chi = \mu_x\sqrt{\lambda}x\left[1-\frac{\lambda}{4}(x^2+y^2)+\frac{\lambda^2}{16}(x^2+y^2)^2-\cdots\right], \tag{37a}$$

$$\mu_{Zy} = \mu_y \sin\theta\sin\chi = \mu_y\sqrt{\lambda}y\left[1-\frac{\lambda}{4}(x^2+y^2)+\frac{\lambda^2}{16}(x^2+y^2)^2-\cdots\right], \tag{37b}$$

$$\mu_{Zz} = \mu_z\cos\theta = \mu_z\left[1-\frac{\lambda}{2}(x^2+y^2)+\frac{\lambda^2}{8}(x^2+y^2)^2-\cdots\right]. \tag{37c}$$

Contributions of each term of Eqs. (37) to transitions can be deduced from Eqs. (20) and (21), and their results are summarized in Table VIII. Matrix elements of the leading terms are as follows:

$$\langle v_x\pm1,v_y,m|\mu_{Zx}|v_x,v_y,m\rangle = \sqrt{\lambda}\mu_x\left[\frac{\sigma_y^{1/2}}{2}\left(v_x+\frac{1}{2}\pm\frac{1}{2}\right)\right]^{1/2}, \tag{38a}$$

$$\langle v_x,v_y\pm1,m|\mu_{Zy}|v_x,v_y,m\rangle = \sqrt{\lambda}\mu_y\left[\frac{\sigma_x^{1/2}}{2}\left(v_y+\frac{1}{2}\pm\frac{1}{2}\right)\right]^{1/2}, \tag{38b}$$

$$\langle v_x,v_y,m|\mu_{Zz}|v_x,v_y,m\rangle = \mu_z. \tag{38c}$$

TABLE VII. Selection rules on $|v_x,v_y,m\rangle$.

Transition dipole	Transition type	Selection rules $(\Delta v_x,\Delta v_y,\Delta m)$
μ_Z	μ_x	(odd, even, 0)
	μ_y	(even, odd, 0)
	μ_z	(even, even, 0)
$\begin{pmatrix}\mu_X\\ \mu_Y\end{pmatrix}$	μ_x	(even, even, ±1) or (odd, odd, ±1)
	μ_y	(even, even, ±1) or (odd, odd, ±1)
	μ_z	(even, odd, ±1) or (odd, even, ±1)

TABLE VIII. Contribution of transition dipole (μ_{Zg}) to transitions.

Transition dipole	Order of λ	Contribution $(|\Delta v_x|,|\Delta v_y|,|\Delta m|)$
μ_{Zx}	$\lambda^{1/2}$	(1,0,0)
	$\lambda^{3/2}$	(1,0,0),(1,2,0),(3,0,0)
	⋮	⋮
μ_{Zy}	$\lambda^{1/2}$	(0,1,0)
	$\lambda^{3/2}$	(0,1,0),(0,3,0),(2,1,0)
	⋮	⋮
μ_{Zz}	λ^0	(0,0,0)
	λ^1	(0,0,0),(0,2,0),(2,0,0)
	⋮	⋮

Similarly, μ_{Xg} is expressed as

$$\mu_{Xx} = \mu_x(\cos\phi\cos\theta\cos\chi-\sin\phi\sin\chi) = \frac{\mu_x}{2}\left[(e^{i\psi}+e^{-i\psi})-\{(x+iy)e^{i\psi}+(x-iy)e^{-i\psi}\}\times\left\{\frac{\lambda}{2}-\frac{\lambda^2}{8}(x^2+y^2)+\cdots\right\}\right], \tag{39a}$$

$$\mu_{Xy} = \mu_y(-\cos\phi\cos\theta\sin\chi-\sin\phi\cos\chi) = \frac{\mu_y}{2}\left[i(e^{i\psi}-e^{-i\psi})-y\{(x+iy)e^{i\psi}+(x-iy)e^{-i\psi}\}\times\left\{\frac{\lambda}{2}-\frac{\lambda^2}{8}(x^2+y^2)+\cdots\right\}\right], \tag{39b}$$

$$\mu_{Xz} = \mu_z\cos\phi\sin\theta = \frac{\mu_z}{2}\sqrt{\lambda}\{(x+iy)e^{i\psi}+(x-iy)e^{-i\psi}\}\times\left[1-\frac{\lambda}{4}(x^2+y^2)+\frac{\lambda^2}{16}(x^2+y^2)^2-\cdots\right]. \tag{39c}$$

Again, contributions of each term of Eqs. (39) to transitions can be deduced as summarized in Table IX. Matrix elements of the leading terms are as follows:

$$\langle v_x,v_y,m\pm1|\mu_{Xx}|v_x,v_y,m\rangle = \frac{\mu_x}{2}, \tag{40a}$$

$$\langle v_x,v_y,m\pm1|\mu_{Xy}|v_x,v_y,m\rangle = \pm i\frac{\mu_y}{2}, \tag{40b}$$

$$\langle v_x+1,v_y,m\pm1|\mu_{Xz}|v_x,v_y,m\rangle = \sqrt{\lambda}\frac{\mu_z}{2}\sqrt{\sigma_y^{1/2}(v_x+1)/2}, \tag{40c}$$

TABLE IX. Contribution of transition dipole (μ_{Xg}) to transitions.

Transition dipole	Order of λ	Contribution ($\|\Delta v_x\|,\|\Delta v_y\|,\|\Delta m\|$)
μ_{Xx}	λ^0	(0,0,1)
	λ^1	(0,0,1),(0,2,1),(2,0,1)
	⋮	⋮
μ_{Xy}	λ^0	(0,0,1)
	λ^1	(0,0,1),(0,2,1),(2,0,1)
	⋮	⋮
μ_{Xz}	$\lambda^{1/2}$	(0,1,1),(1,0,1)
	$\lambda^{3/2}$	(0,1,1),(0,3,1),(1,0,1), (1,2,1),(2,1,1),(3,0,1)
	⋮	⋮

$$\langle v_x-1,v_y,m\pm1|\mu_{Xz}|v_x,v_y,m\rangle=\sqrt{\lambda}\frac{\mu_z}{2}\sqrt{\sigma_y^{1/2}v_x/2}, \tag{40d}$$

$$\langle v_x,v_y+1,m\pm1|\mu_{Xz}|v_x,v_y,m\rangle=i\sqrt{\lambda}\frac{\mu_z}{2}\sqrt{\sigma_x^{1/2}(v_y+1)/2}, \tag{40e}$$

$$\langle v_x,v_y-1,m\pm1|\mu_{Xz}|v_x,v_y,m\rangle=-i\sqrt{\lambda}\frac{\mu_z}{2}\sqrt{\sigma_x^{1/2}v_y/2}. \tag{40f}$$

F. Calculations of transition intensity

The transition intensity is obtained by

$$\left|\int|\Psi^f\rangle^*\mu_F|\Psi^i\rangle d\mathbf{v}\right|^2=\left|\langle\Psi^f|\left(1+\frac{x^2+y^2}{4}\lambda\right)^{-2}\mu_F|\Psi^i\rangle\right|^2, \tag{41}$$

where $[1+(x^2+y^2)\lambda/4]^{-2}$ is expanded as

$$\left(1+\frac{x^2+y^2}{4}\lambda\right)^{-2}=1-\frac{x^2+y^2}{2}\lambda+\frac{3(x^2+y^2)^2}{16}\lambda^2-\cdots. \tag{42}$$

$|\Psi\rangle$ is composed of zeroth-order wave functions,

$$|\Psi^i\rangle=|i\rangle+\lambda\sum_s C_{i,s}^{(1)}|s\rangle+\lambda^2\sum_s C_{i,s}^{(2)}|s\rangle+\cdots, \tag{43}$$

where the index s denotes a set of (v_x,v_y,m). $C_{i,s}^{(n)}$ is the coefficient of nth-order wave function derived by the perturbation theory. The transition dipole operators, which appear in Eqs. (37) and (39), are also expanded into the power series of λ, and we formally express them as follows:

$$\mu_{Fg}=\mu_{Fg}^{(0)}+\lambda\mu_{Fg}^{(1)}+\lambda^2\mu_{Fg}^{(2)}+\cdots \tag{44}$$

for μ_{Zz}, μ_{Xx}, or μ_{Xy}, and

$$\mu_{Fg}=\lambda^{1/2}\mu_{Fg}^{(1/2)}+\lambda^{3/2}\mu_{Fg}^{(3/2)}+\lambda^{5/2}\mu_{Fg}^{(5/2)}+\cdots \tag{45}$$

for μ_{Zx}, μ_{Zy}, or μ_{Xz}. We call the situations of $\langle f|\mu_{Fg}^{(0)}|i\rangle\neq0(=0)$ and $\langle f|\mu_{Fg}^{(1/2)}|i\rangle\neq0(=0)$ as the allowed (forbidden) transitions at the lowest order. When a transition is forbidden at the lowest order, the leading contributions to the transition strength are the order of λ^2 or λ^3 for Eq. (44) type or Eq. (45) type transitions, respectively.

As depicted in Eq. (13), the zeroth-order wave function depends on the rotational constants $\sigma_{x,y}$. On the other hand, x and y are dependent on the parameter λ, see Eqs. (6) and (7a). Thus, if a final state has different $\sigma_{x,y}$ or λ from those of an initial state, analytical representations of matrix elements, like Eqs. (20) and (21), cannot be applied. Up to this point, therefore, we have assumed that $\sigma_{x,y}$ and λ do not change between the initial and final states. However, sometimes this approximation does not hold, in particular for electronic transitions. We discuss the method for such cases in the restriction that the direction of μ does not change.

We introduce parameters d_x and d_y as follows:

$$d_x=\frac{\lambda_i\sqrt{\sigma_y^i}-\lambda_f\sqrt{\sigma_y^f}}{\lambda_i\sqrt{\sigma_y^i}+\lambda_f\sqrt{\sigma_y^f}}, \tag{46a}$$

$$d_y=\frac{\lambda_i\sqrt{\sigma_x^i}-\lambda_f\sqrt{\sigma_x^f}}{\lambda_i\sqrt{\sigma_x^i}+\lambda_f\sqrt{\sigma_x^f}}, \tag{46b}$$

where i and f stand for initial and final states, respectively. $d_{x,y}$ ranges $-1<d_{x,y}<1$, and $d_{x,y}$ equals to zero if $\sigma_{x,y}$ and λ do not change. In the case of $\sigma_x^i=\sigma_x^f$ and $\sigma_y^i=\sigma_y^f$, d_x is identical to d_y. Additional new parameters σ_x and σ_y are defined as

$$\sigma_x=\left[\frac{(\lambda_i+\lambda_f)\sqrt{\sigma_x^i\sigma_x^f}}{\lambda_i\sqrt{\sigma_x^i}+\lambda_f\sqrt{\sigma_x^f}}\right]^2, \tag{47a}$$

$$\sigma_y=\left[\frac{(\lambda_i+\lambda_f)\sqrt{\sigma_y^i\sigma_y^f}}{\lambda_i\sqrt{\sigma_y^i}+\lambda_f\sqrt{\sigma_y^f}}\right]^2. \tag{47b}$$

Using the above parameters, new variables x, y are defined as

$$\frac{x_i}{(\sigma_y^i)^{1/4}}=(1-d_x)^{1/2}\frac{x}{\sigma_y^{1/4}}, \tag{48a}$$

$$\frac{y_i}{(\sigma_x^i)^{1/4}}=(1-d_y)^{1/2}\frac{y}{\sigma_x^{1/4}}. \tag{48b}$$

Then, x_f and y_f yield

$$\frac{x_f}{(\sigma_y^f)^{1/4}}=(1+d_x)^{1/2}\frac{x}{\sigma_y^{1/4}}, \tag{49a}$$

$$\frac{y_f}{(\sigma_x^f)^{1/4}}=(1+d_y)^{1/2}\frac{y}{\sigma_x^{1/4}}. \tag{49b}$$

Making use of the relation of Eq. (B4), $|v_x^i,v_y^i,m^i\rangle$, which is a function of x_i, y_i, and ψ, is transformed into

$$|v_x^i,v_y^i,m^i\rangle=\exp\left[\frac{d_x x^2}{2\sigma_y^{1/2}}+\frac{d_y y^2}{2\sigma_x^{1/2}}\right]N_{v_x^i,v_y^i}\sum_{p=0}^{v_x^i}\sum_{q=0}^{v_y^i}(N_{p,q})^{-1}\frac{v_x^i!\,v_y^i!}{p!\,(v_x^i-p)!\,q!\,(v_y^i-q)!}$$
$$\times[2\{(1-d_x)^{1/2}-1\}]^{v_x^i-p}[2\{(1-d_y)^{1/2}-1\}]^{v_y^i-q}\left(\frac{x}{\sigma_y^{1/4}}\right)^{v_x^i-p}\left(\frac{y}{\sigma_x^{1/4}}\right)^{v_y^i-q}|p,q,m^i\rangle, \tag{50}$$

where $|p,q,m^i\rangle$ is a function of x, y, and ψ. Similarly, $|v_x^f,v_y^f,m^f\rangle$ yields

$$|v_x^f,v_y^f,m^f\rangle=\exp\left[-\frac{d_x x^2}{2\sigma_y^{1/2}}-\frac{d_y y^2}{2\sigma_x^{1/2}}\right]N_{v_x^f,v_y^f}\sum_{p=0}^{v_x^f}\sum_{q=0}^{v_y^f}(N_{p,q})^{-1}\frac{v_x^f!\,v_y^f!}{p!\,(v_x^f-p)!\,q!\,(v_y^f-q)!}$$
$$\times[2\{(1+d_x)^{1/2}-1\}]^{v_x^f-p}[2\{(1+d_y)^{1/2}-1\}]^{v_y^f-q}\left(\frac{x}{\sigma_y^{1/4}}\right)^{v_x^f-p}\left(\frac{y}{\sigma_x^{1/4}}\right)^{v_y^f-q}|p,q,m^f\rangle. \tag{51}$$

Because μ_{Fg} does not contain any differential operator, the exponential factors of $\exp[\pm d_x x^2/(2\sigma_y^{1/2})\pm d_y y^2/(2\sigma_x^{1/2})]$ in Eqs. (50) and (51) are canceled by each other in calculations of $\langle v_x^f,v_y^f,m^f|\mu_{Fg}|v_x^i,v_y^i,m^i\rangle$. Then, we can derive $\langle f|\mu_{Fg}|i\rangle$ even in the case that $\sigma_{x,y}$ and λ change at the transitions. It should be noted that $|p,q,m\rangle$ in Eqs. (50) and (51) corresponds to the pendular-state wave functions for $\sigma_{x,y}$ defined in Eqs. (47) and λ represented as

$$\lambda=\frac{2\lambda_i\lambda_f}{\lambda_i+\lambda_f}. \tag{52}$$

In ordinary circumstances, $|d_{x,y}|\ll 1$ is satisfied, and then

$$[2\{(1\pm d_x)^{1/2}-1\}]^{v_x^f-p}[2\{(1\pm d_y)^{1/2}-1\}]^{v_y^f-q}$$
$$\approx(\pm d_x)^{v_x-p}(\pm d_y)^{v_y-q}. \tag{53}$$

Therefore, the series through about p and q can be truncated with a good accuracy.

G. General asymmetric top

In the case of pendular states of a general asymmetric top whose μ is not parallel to any principal axis of inertia, the method described above should be revised. Since the framework of the discussion is almost the same, we just outline the procedures.

First, the principal axes of inertia are transformed to a new molecular-fixed axis system, where the z axis is parallel to μ, by the axis rotation in Euler angles (ϕ_0,θ_0,χ_0). Then Hamiltonian of the asymmetric top is expressed as

$$\hat{H}=\sigma_x\hat{j}_x^2+\sigma_y\hat{j}_y^2+\sigma_z\hat{j}_z^2-\frac{2}{\lambda^2}\cos\theta+c_{yz}(\hat{j}_y\hat{j}_z+\hat{j}_z\hat{j}_y)$$
$$+c_{zx}(\hat{j}_z\hat{j}_x+\hat{j}_x\hat{j}_z), \tag{54}$$

where $\sigma_{x,y,z}$, c_{yz}, c_{zx}, and λ depend on the constant angles of (ϕ_0,θ_0,χ_0). Because only ϕ_0 and θ_0 are sufficient to define the new z axis, the arbitrary angle χ_0 is fixed so as to eliminate the $\hat{j}_x\hat{j}_y$ cross term in the derivation of Eq. (54). After the variable transformation of Eqs. (6) and the expansion of $\hat{H}$ into a power series of λ, we obtain the terms of the order of λ^{-2}, λ^{-1}, λ^0, and λ^n $(n=1,2,3,\ldots)$ identical to Eqs. (9), (10), (23), and (31), respectively. Therefore, zeroth-order energy and wave functions are the same as those discussed in Sec. II A. However, terms of the $\lambda^{-1/2}$ and $\lambda^{1/2}$ order appear in the power series of λ, and expressed as

$$\hat{H}_{\lambda^{-1/2}}=\frac{1}{\sqrt{\lambda}}[c_{zx}\{\hat{p}_y(\hat{j}_Z-\hat{l})+(\hat{j}_Z-\hat{l})\hat{p}_y\}-c_{yz}\{\hat{p}_x(\hat{j}_Z-\hat{l})$$
$$+(\hat{j}_Z-\hat{l})\hat{p}_x\}], \tag{55a}$$

$$\hat{H}_{\lambda^{1/2}}=\frac{\sqrt{\lambda}}{4}[c_{zx}\{(2x\hat{j}_Z-x\hat{l}+y\hat{u})(\hat{j}_Z-\hat{l})+(\hat{j}_Z-\hat{l})(2x\hat{j}_Z-x\hat{l}$$
$$+y\hat{u})\}-c_{yz}\{(2y\hat{j}_Z-y\hat{l}-x\hat{u})(\hat{j}_Z-\hat{l})+(\hat{j}_Z-\hat{l})$$
$$\times(2y\hat{j}_Z-y\hat{l}-x\hat{u})\}]. \tag{55b}$$

Because all the diagonal matrix elements of $\hat{H}_{\lambda^{-1/2}}$ are zero, $\hat{H}_{\lambda^{-1/2}}$ has no effect on energy levels in first order. Thus, the most influential energy correction is the order of λ^0, and represented as

$$E_{v_x,v_y,m}(\lambda^0)=-\left[\frac{\sigma_y}{8}+\frac{3c_{yz}^2}{2\sigma_y}\cdot\frac{\sigma_y-\sigma_x}{4\sigma_y-\sigma_x}\right]\left(v_x+\frac{1}{2}\right)^2-\left[\frac{\sigma_x}{8}\right.$$
$$+\left.\frac{3c_{zx}^2}{2\sigma_x}\cdot\frac{\sigma_x-\sigma_y}{4\sigma_x-\sigma_y}\right]\left(v_y+\frac{1}{2}\right)^2+\left[\frac{1}{2}\left(\frac{4\sigma_z}{\sigma_x^{1/2}\sigma_y^{1/2}}\right.\right.$$
$$\left.-3\sigma_x^{1/2}\sigma_y^{1/2}\right)-\frac{4}{\sigma_x^{1/2}\sigma_y^{1/2}}\left(c_{yz}^2\frac{\sigma_y+2\sigma_x}{4\sigma_y-\sigma_x}\right.$$
$$\left.\left.+c_{zx}^2\frac{\sigma_x+2\sigma_y}{4\sigma_x-\sigma_y}\right)\right]\left(v_x+\frac{1}{2}\right)\left(v_y+\frac{1}{2}\right)+\left[\sigma_z-\frac{c_{zx}^2}{\sigma_x}\right.$$
$$\left.-\frac{c_{yz}^2}{\sigma_y}\right]m^2-\frac{\sigma_z}{2}-\frac{1}{16}+\frac{3}{8}\left(\frac{c_{yz}^2}{\sigma_y}\cdot\frac{5\sigma_y+\sigma_x}{4\sigma_y-\sigma_x}\right.$$
$$\left.+\frac{c_{zx}^2}{\sigma_x}\cdot\frac{5\sigma_x+\sigma_y}{4\sigma_x-\sigma_y}\right). \tag{56}$$

TABLE X. Character table for a general asymmetric top in a uniform external field.

	E	$C^Z(\delta)$	$C^Z(-\delta)$
$\phi\rightarrow$	ϕ	$\phi+\delta$	$\phi-\delta$
$\psi\rightarrow$	ψ	$\psi+\delta$	$\psi-\delta$
0	1	1	1
M^+	1	$e^{iM\delta}$	$e^{-iM\delta}$
M^-	1	$e^{-iM\delta}$	$e^{iM\delta}$

The symmetry group should be also revised. Because the symmetry operations are only E and $C^Z(\pm\delta)$, the character table of a general asymmetric top in a uniform external field becomes as shown in Table X. While M^+ and M^- are distinct irreducible representations, the time reversal symmetry causes an extra degeneracy between M^+ and M^-, called a separably degenerate. The selection rule is rather trivial: transitions of μ_X and μ_Y are $\Delta m=\pm 1$, and a transition of μ_Z is $\Delta m=0$.

III. SYMMETRIC TOP IN PENDULAR STATES

In this section, we describe a theory of pendular-state spectroscopy for symmetric-top molecules. Since an analytical representation of energy levels for symmetric-top molecules in the pendular limit was reported previously [35], we mainly describe symmetries, selection rules, and transition intensities, which are newly derived in this study. Because a modification of the theory into a linear-rotor version is straightforward, it is not mentioned in the following discussions.

A. Energy levels and wave functions

For the purpose of a consistent description throughout this paper, we show analytical representations of wave functions and energy levels for symmetric-top molecules in the pendular limit, whose expressions are slightly different from the previous ones [35].

The similar procedure to the case of an asymmetric top gives $\hat{H}_{\lambda^{-2}}$ as Eq. (9). The term of λ^{-1} is

$$\hat{H}_{\lambda^{-1}} = \lambda^{-1}\left[-\frac{1}{r}\frac{\partial}{\partial r}\left(r\frac{\partial}{\partial r}\right)-\frac{1}{r^2}\frac{\partial^2}{\partial\rho^2}+r^2\right] = \lambda^{-1}[\hat{p}_+\hat{p}_- + r_+r_-] = \lambda^{-1}\hat{h}_0^s, \tag{57}$$

where r, ρ, and ψ have been defined in Eqs. (7a), (7b), and (6a), respectively. $r_\pm$, $\hat{p}_\pm$, and $\hat{l}$ are defined as

$$r_\pm = re^{\pm i\rho}, \tag{58a}$$

$$\hat{p}_\pm = e^{\pm i\rho}\left(-i\frac{\partial}{\partial r}\pm\frac{i}{r}\hat{l}\right), \tag{58b}$$

$$\hat{l} = -i\frac{\partial}{\partial\rho}. \tag{58c}$$

The form of Eq. (57) shows that the zeroth-order representation of a pendular-state symmetric top is a two-dimensional isotropic harmonic oscillator. Then, the zeroth-order energy is expressed as

$$E^{(0)}_{v,l,m} = 2(v+1). \tag{59}$$

As shown in Eq. (59), the zeroth-order energy is determined by only a vibrational quantum number v.

The zeroth-order wave functions are expressed as

$$|v,l,m\rangle = N_{v,l}r^{|l|}e^{-r^2/2}L^{|l|}_{(v+|l|)/2}(r^2)e^{il\rho}e^{im\psi}, \tag{60}$$

where $L^p_q(\xi)$ is an associated Laguerre polynomial, and l is a quantum number for the vibrational angular momentum, i.e.,

$$\hat{l}|v,l,m\rangle = l|v,l,m\rangle. \tag{61}$$

We choose $e^{im\psi}$ for an arbitrary function of ψ for the similar reason discussed in Sec. II A. The constant $N_{v,l}$ is defined as

$$N_{v,l} = \sqrt{\frac{\left(\frac{v-|l|}{2}\right)!}{2\lambda\pi^2\left[\left(\frac{v+|l|}{2}\right)!\right]^3}}, \tag{62}$$

$\hat{l}$ of Eq. (58c) is identical to the operator defined by Eq. (24a). $\hat{l}$ is expressed as

$$\hat{l} = \hat{j}_Z - \hat{j}_z \tag{63}$$

and the vibrational quantum number l satisfies

$$l = m - k, \tag{64}$$

where k is a projection of angular momentum, j, in the field-free condition on the molecular z axis. The basis of $|v,l,m\rangle$ is not orthonormal in the same manner of asymmetric tops, and this problem can be handled by a similar way described in Sec. II A.

The λ^0 term of the Hamiltonian is represented as

$$\hat{H}_{\lambda^0} = \frac{r^2}{2}\hat{h}_s^0 - \frac{3}{4}r^4 + \sigma_z\hat{j}_Z^2 - (2\sigma_z-1)\hat{l}\hat{j}_Z + (\sigma_z-1)\hat{l}^2 \tag{65}$$

and the first-order correction to the energy is expressed as

$$E_{v,l,m}(\lambda^0) = -\tfrac{1}{8}(v+1)^2 + \sigma_z m^2 - (2\sigma_z-1)ml + (\sigma_z-\tfrac{5}{8})l^2 - \tfrac{3}{8}, \tag{66}$$

$E_{v,l,m}(\lambda^0)$ provides the energy-level splittings about m and l.

B. Symmetry considerations

In this section, we describe a symmetry group appropriate to a symmetric top in a uniform electric field. In the case of a symmetric top, an arbitrary rotation around the z axis is a symmetry operation. Here we denote $C_z(\delta)$ as the rotation by an angle of δ. Then, Euler angles are transformed by $C_z(\delta)$ as $(\phi,\theta,\chi)\rightarrow(\phi,\theta,\chi+\delta)$. Next, we introduce π rotations about

TABLE XI. Character table for a symmetric top in a uniform external field.

	E	$C^Z(\delta+\gamma)C_z(-\gamma)$ $C^Z(-\delta-\gamma)C_z(\gamma)$	$C_\alpha^{\perp Z}(\pi)C_\beta^{\perp z}(\pi)$	
$\phi\rightarrow$	ϕ	$\phi\pm(\delta+\gamma)$	$\pi-\phi+2\alpha$	
$\chi\rightarrow$	χ	$\chi\mp\gamma$	$-\chi+2\beta$	
$\psi\rightarrow$	ψ	$\psi\pm\delta$	$\pi-\psi+2\alpha+2\beta$	
$\rho\rightarrow$	ρ	$\rho\pm\gamma$	$-\phi+2\beta$	
$(0,0)^+$	1	1	1	z, r
$(0,0)^-$	1	1	-1	$\hat{j}_Z$, $\hat{j}_z$
$(0,L)^a$	2	$2\cos L\gamma$	0	
$(M,0)^b$	2	$2\cos M\delta$	0	
$(M,L)^{+a,b}$	2	$2\cos(M\delta+L\gamma)$	0	
$(M,L)^{-a,b}$	2	$2\cos(M\delta-L\gamma)$	0	

[a] $L=1,2,3,\ldots$.
[b] $M=1,2,3,\ldots$.

an arbitrary axis in the xy plane, $C_\alpha^{\perp z}(\pi)$, where α stands for the angle measured from the x axis to the rotation axis in the xy plane. Then, the operations of $C_\alpha^{\perp Z}(\pi)C_\beta^{\perp z}(\pi)$ become symmetry operations for arbitrary angles of α and β, and Euler angles are transformed as $(\phi,\theta,\chi)\rightarrow(\pi-\phi+2\alpha,\theta,-\chi+2\beta)$. As a result, symmetry operations are as follows:

$$\{E,C^Z(\delta)C_z(\gamma),C_\alpha^{\perp Z}(\pi)C_\beta^{\perp z}(\pi)\}, \tag{67}$$

where α and β are arbitrary angles, and likewise, δ and γ are arbitrary angles except $\delta=\gamma=0$. After the classification of these operators with the similar procedure to Eq. (28), the character table for a symmetric top in a uniform electric field is derived as listed in Table XI. Symmetries of z, r, $\hat{j}_Z$, and $\hat{j}_z$ are also depicted in the table. Symmetries of the other operators are $(0,1)$ for (x,y), $(\hat{j}_x,\hat{j}_y)$, (r_+,r_-), and $(\hat{p}_+,\hat{p}_-)$, $(0,0)^+$ for $r_\pm\hat{p}_\mp$, and so on. Table XII shows that the zeroth-order wave function of Eq. (60) is an irreducible representation. It is noted that the pair of $|v,l,m\rangle$ and $|v,-l,-m\rangle$ forms a doubly degenerated representation except for the $m=l=0$ states.

The symmetrized basis set of a free rotating symmetric top is expressed as follows:

$$\text{(i) } m=k=0:|j,0,0\rangle_f, \tag{68a}$$

$$\text{(ii) } m\neq 0 \text{ or } k\neq 0:\begin{pmatrix}|j,k,m\rangle_f\\ |j,-k,-m\rangle_f\end{pmatrix}. \tag{68b}$$

We can easily derive the symmetry of a field-free basis of Eqs. (68) with the relation of Eq. (64). The results are shown in Table XIII. The symmetry correlation between the pendular-state and the field-free energy levels is also obtained by the relation of Eq. (64).

In the free rotation of a symmetric top, the energy ordering of the same (k,m) levels are explicitly determined, i.e., the higher j state is in higher energy. In the pendular limit, on the other hand, the energy ordering of the same (l,m) levels are also determined, i.e., the higher v state is in higher energy. Thus, an adiabatic symmetry correlation between the quantum number in a free rotation, j, and that in the pendular limit, v, can be derived using the relation of Eq. (64). In the pendular condition, the approximate quantum number, v, is represented as

TABLE XII. Symmetry of pendular-limit wave function, $|v,l,m\rangle$.

m,l	Symmetry
$m=0$, $l=0$	$(0,0)^+$
$m=0$, $l\neq 0$	$(0,\lvert l\rvert)$
$m\neq 0$, $l=0$	$(\lvert m\rvert,0)$
$m\cdot l>0$	$(\lvert m\rvert,\lvert l\rvert)^+$
$m\cdot l<0$	$(\lvert m\rvert,\lvert l\rvert)^-$

$$v=|l|+2n, \tag{69}$$

where $n=0,1,2,\ldots$ is a numbering of eigenstates counted from the lowest state in a $(|m|,|l|)^\pm$ levels. Using the number, n, the angular momentum quantum number in the field-free condition is expressed as

$$j=\frac{|m+k|+|m-k|}{2}+n. \tag{70}$$

Therefore, the correlation between (v,l,m) and (j,k,m) are represented as

$$v=2j-|m+k|, \tag{71}$$

$$l=m-k. \tag{72}$$

This explicit correspondence enables us to label the eigenstates in terms of (v,l,m) or (j,k,m) in arbitrary fields. The identical correlation has been reported for linear rotors [32,34] and for symmetric tops [35].

Finally, a symmetry correlation between symmetric tops and asymmetric tops is discussed. Because the symmetry operations of symmetric-top molecules include those of asymmetric-top molecules, a symmetry correlation between symmetric- and asymmetric-top molecules can be obtained, and the results are shown in Table XIV.

C. Nonperturbative treatments

A new approach similar to the method discussed in Sec. II D is available. An orthonormal pendular basis set is represented as

TABLE XIII. Symmetry of the field-free basis.

Configuration	Symmetry
$m=0$, $k=0$	$(0,0)^+$
$m=0$, $k\neq 0$	$(0,\lvert k\rvert)$
$m\neq 0$, $k=m$	$(\lvert m\rvert,0)$
$m\cdot(m-k)>0$	$(\lvert m\rvert,\lvert m-k\rvert)^+$
$m\cdot(m-k)<0$	$(\lvert m\rvert,\lvert m-k\rvert)^-$

TABLE XIV. Symmetry correlation between symmetric and asymmetric tops.

Symmetric tops	Asymmetric tops
$(0,0)^+$	$(0^+,A)$
$(0,0)^-$	$(0^-,A)$
$(0,L)$, L=even	$(0^+,A)\oplus(0^-,A)$
$(0,L)$, L=odd	$(0^+,B)\oplus(0^-,B)$
$(M,0)$, M=even	(M,A)
$(M,0)$, M=odd	(M,B)
$(M,L)^{\pm}$, $M+L$=even	(M,A)
$(M,L)^{\pm}$, $M+L$=odd	(M,B)

$$|v,l,m\rangle_{\text{o.n.}} = \left(1+\frac{r^2}{4}\lambda\right)|v,l,m\rangle, \tag{73}$$

where $|v,l,m\rangle$ is defined in Eq. (60). In the similar way to the asymmetric-top case, matrix elements of the full Hamiltonian are numerically calculated by Gauss-Laguerre quadratures, and diagonalization of the obtained Hamiltonian matrix gives energy levels and wave functions represented by the orthonormal pendular basis set. Because the adiabatic quantum number correlation between a free rotation and the pendular limit is definite in the case of symmetric tops, as shown in Eqs. (71) and (72), the assignment on the pendular-state quantum numbers is straightforward from Eq. (69) even in the matrix diagonalization method with the free-rotation basis set. In this respect, the method using the free-rotation basis set is easier to utilize than the method using the orthonormal pendular basis set.

D. Selection rules

The transition dipole operator, $\mu_F(F=X,Y,Z)$, is the same as that discussed in Sec. II E. Therefore, the transformation property of μ_F is derived from the Euler angle transformations in Table XI. The resultant transformation property determines the symmetry of μ_F as shown in Table XV. It is worth noting that the x,y components of (μ_X,μ_Y) forms reducible representation, and can be divided into two irreducible representations, $(1,0)$ and $(1,2)^+$. Hereafter, $(1,0)$ part of μ_{Fg} is denoted as $\mu_{Fg}^{(1,0)}$, and $\mu_{Fg}^{(1,2)^+}$ stands for the $(1,2)^+$ part, where $F=X,Y$ and $g=x,y$. Because it is arbitrary to determine the x and y axes in the case of a symmetric top, the pair of μ_{Fx} and μ_{Fy} is doubly degenerate; see Table XV.

TABLE XV. Symmetries of transition dipoles.

Transition dipole	Transition type	Symmetry
μ_Z	(μ_x,μ_y)	$(0,1)$
	μ_z	$(0,0)$
$\begin{pmatrix}\mu_X\\ \mu_Y\end{pmatrix}$	(μ_x,μ_y)	$(1,0)\oplus(1,2)^+$
	μ_z	$(1,1)^+$

TABLE XVI. Selection rules on $|v,l,m\rangle$.

Transition dipole	Transition type	Selection rule $(\Delta m,\Delta l)$
μ_Z	(μ_x,μ_y)	$(0,\pm1)$
	μ_z	$(0,0)$
$\begin{pmatrix}\mu_X\\ \mu_Y\end{pmatrix}$	$(1,0)$ part of (μ_x,μ_y)	$(\pm1,0)$
	$(1,2)^+$ part of (μ_x,μ_y)	$(\pm1,\pm2)$
	μ_z	$(\pm1,\pm1)$

Thus, considerations about only μ_{Fx} are sufficient, where $F=X,Y,Z$. In the light of symmetries of zeroth-order wave functions discussed in Sec. III B, the selection rules in terms of $|v,l,m\rangle$ can be derived as depicted in Table XVI.

The representations for μ_{Fg} are as follows:

$$\mu_{Zx} = \frac{\sqrt{\lambda}}{2}\mu_x(e^{i\rho}+e^{-i\rho})r\left[1-\frac{\lambda}{4}r^2+\cdots\right], \tag{74a}$$

$$\mu_{Zz} = \mu_z\left[1-\frac{\lambda}{2}r^2+\cdots\right], \tag{74b}$$

$$\mu_{Xx}^{(1,0)} = \frac{1}{4}\mu_x(e^{i\psi}+e^{-i\psi})\left[2-\frac{\lambda}{2}r^2+\cdots\right], \tag{74c}$$

TABLE XVII. Contribution of transition dipole (μ_{Fg}) to transitions.

Transition dipole	Order of λ	Contribution $(\lvert\Delta v\rvert,\Delta l,\Delta m)$
μ_{Zx}	$\lambda^{1/2}$	$(1,\pm1,0)$
	$\lambda^{3/2}$	$(1,\pm1,0),(3,\pm1,0)$
	$\lambda^{5/2}$	$(1,\pm1,0),(3,\pm1,0),(5,\pm1,0)$
	⋮	⋮
μ_{Zz}	λ^0	$(0,0,0)$
	λ^1	$(0,0,0),(2,0,0)$
	λ^2	$(0,0,0),(2,0,0),(4,0,0)$
	⋮	⋮
$\mu_{Xx}^{(1,0)}$	λ^0	$(0,0,\pm1)$
	λ^1	$(0,0,\pm1),(2,0,\pm1)$
	λ^2	$(0,0,\pm1),(2,0,\pm1),(4,0,\pm1)$
	⋮	⋮
$\mu_{Xx}^{(1,2)^+}$	λ^1	$(0,\pm2,\pm1),(2,\pm2,\pm1)$
	λ^2	$(0,\pm2,\pm1),(2,\pm2,\pm1),(4,\pm2,\pm1)$
	⋮	⋮
μ_{Xy}	$\lambda^{1/2}$	$(1,\pm1,\pm1)$
	$\lambda^{3/2}$	$(1,\pm1,\pm1),(3,\pm1,\pm1)$
	$\lambda^{5/2}$	$(1,\pm1,\pm1),(2,\pm1,\pm1),(5,\pm1,\pm1)$
	⋮	⋮

$$\mu_{Xx}^{(1,2)^+} = \frac{1}{4}\mu_x(e^{i(\psi+2\rho)} + e^{-i(\psi+2\rho)})\left[\frac{\lambda}{2}r^2 - \frac{\lambda^2}{8}r^4 + \cdots\right], \tag{74d}$$

$$\mu_{Xz} = -\frac{\sqrt{\lambda}}{2}\mu_z(e^{i(\psi+\rho)} + e^{-i(\psi+\rho)})r\left[1 - \frac{\lambda}{4}r^2 + \cdots\right]. \tag{74e}$$

Contributions of each term of Eqs. (74) to transitions are summarized in Table XVII. The leading terms of $\langle v^f, l^f, m^f|\mu_{Fg}|v^i, l^i, m^i\rangle$ are as follows:

$$\langle v+1, l\pm 1, m|\mu_{Zx}|v,l,m\rangle = \sqrt{\lambda}\frac{\mu_x}{2}\sqrt{\frac{v\pm l+2}{2}}, \tag{75a}$$

$$\langle v-1, l\pm 1, m|\mu_{Zx}|v,l,m\rangle = \sqrt{\lambda}\frac{\mu_x}{2}\sqrt{\frac{v\mp l}{2}}, \tag{75b}$$

$$\langle v, l\pm 1, m|\mu_{Zz}|v,l,m\rangle = \mu_z, \tag{75c}$$

$$\langle v, l, m\pm 1|\mu_{Xx}^{(1,0)}|v,l,m\rangle = \frac{\mu_x}{2}, \tag{75d}$$

$$\langle v+1, l\pm 1, m\pm 1|\mu_{Xz}|v,l,m\rangle = -\sqrt{\lambda}\frac{\mu_z}{2}\sqrt{\frac{v\pm l+2}{2}}, \tag{75e}$$

$$\langle v-1, l\pm 1, m\pm 1|\mu_{Xz}|v,l,m\rangle = -\sqrt{\lambda}\frac{\mu_z}{2}\sqrt{\frac{v\mp l}{2}}. \tag{75f}$$

Calculations of transition strength are carried out with the same procedure discussed in Sec. II F. In the situations that λ changes in a transition, a similar discussion to Sec. II F is possible, and we describe it briefly. A new variable r is introduced by

$$r_i = (1-d)^{1/2}r, \tag{76a}$$

$$r_f = (1+d)^{1/2}r. \tag{76b}$$

Then, d satisfies

$$d = \frac{\lambda_i - \lambda_f}{\lambda_i + \lambda_f}. \tag{77}$$

Using the relation of Eq. (B8), $|v^i, l^i, m^i\rangle$, which is a function of r_i, ρ, and ψ, yields

$$|v^i, \pm|l^i|, m^i\rangle = e^{dr^2/2}N_{v^i,l^i}(1-d)^{|l^i|/2}\sum_{p=0}^{(v^i-|l^i|)/2}\left[(N_{v^i-p,|l^i|+p})^{-1}\frac{(-d)^p}{p!}(r_\mp)^p|v^i-p, \pm(|l^i|+p), m^i\rangle\right], \tag{78}$$

where $r_\pm$ is defined in Eq. (58a), and $|v^i-p, \pm(|l^i|+p), m^i\rangle$ is a function of r, ρ, and ψ. Similarly, $|v^f, l^f, m^f\rangle$ becomes

$$|v^f, \pm|l^f|, m^f\rangle = e^{-dr^2/2}N_{v^f,l^f}(1+d)^{|l^f|/2}\sum_{p=0}^{(v^f-|l^f|)/2}\left[(N_{v^f-p,|l^f|+p})^{-1}\frac{d^p}{p!}(r_\mp)^p|v^f-p, \pm(|l^f|+p), m^f\rangle\right]. \tag{79}$$

The wave functions $|v-p, \pm(|l|+p), m\rangle$ in Eqs. (78) and (79) correspond to those for λ defined as Eq. (52). From the same reason discussed in Sec. II F, the factor of $e^{dr^2/2}$ in Eq. (78) and $e^{-dr^2/2}$ in Eq. (79) are canceled out to each other in calculations of $\langle v^f, l^f, m^f|\mu_{Fg}|v_x^i, v_y^i, m^i\rangle$, and the series through about k can be truncated with a good accuracy in the case of $|d| \ll 1$. Therefore, the calculation of the transition oscillator strength becomes possible.

IV. UTILITY OF THE PENDULAR-LIMIT FORMALISM

In this section, we show usefulness of the present analytical expressions. Numerical calculations of energy levels and spectra for molecules in pendular states are carried out with the matrix diagonalization method, which provides practically exact results, and they are compared with results from the analytical representation. We demonstrate that gross features of energy levels and spectra in pendular states are well reproduced by the analytical representations, and assignments of states and transitions are easily performed in terms of pendular-state quantum numbers.

A. Energy levels

Energy-level representation of asymmetric-top molecules in a strong-field limit is shown in Eq. (26). Since the correspondence between the (x,y,z) axis and the (a,b,c) axis depends on the direction of μ, energy levels change not only with $\sigma_{x,y,z}$ but also with the direction of μ. Suppose an asymmetric top molecule of which μ directs to the b axis, the x and y axes correspond to the c and a axes, respectively. This type of molecules represents the nature of pendular states of asymmetric tops most clearly because of the large difference between σ_x and σ_y (note $\sigma_x = \sigma_y$ in the symmetric-top case). Therefore, molecules with $\mu \| b$ can be regarded as a typical model for an asymmetric top in a pendular state. Figure 2(a)

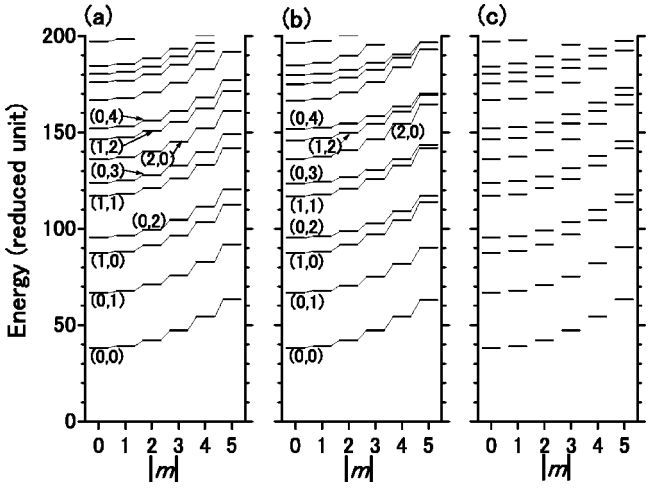

FIG. 2. Energy levels of an asymmetric top reproduced by (a) the analytical representation, (b) the analytical representation with the second-order energy correction, and (c) the matrix diagonalization method. The energy levels of different $|m|$ are separately depicted. The model parameters are described in the text. Levels with the same v_x, v_y are denoted as (v_x, v_y) and connected by thin lines in (a) and (b). All energies are measured from the potential minimum of $-2/\lambda^2 = -800.0$.

shows the energy levels derived from Eq. (26) for a molecule with $\mu \| b$, where $\sigma_x = 0.5$, $\sigma_y = 1.5$, $\sigma_z = 1.0$, and $\lambda = 0.05$. All energies are expressed in a unit reduced by the averaged rotational constant, $(\mathcal{B}_x + \mathcal{B}_y)/2 = (C+A)/2$. In this condition, the fundamental frequencies of pendular vibrations along the x and y axes are $2\sigma_y^{1/2}/\lambda \approx 49.0$ and $2\sigma_x^{1/2}/\lambda \approx 28.3$, respectively. The zero-point shift is $-2/\lambda^2 = -800$, and Ray's asymmetry parameter, κ, is zero. In lower-energy region, levels with the same v_x, v_y are represented as (v_x, v_y) and connected by thin lines in Fig. 2(a). The results of numerical calculations with the matrix diagonalization method using the free-rotation basis set are depicted in Fig. 2(c), where the energy levels are regarded as accurate. Comparing Figs. 2(a) and 2(c), the analytical representation of Eq. (26) reproduces reasonably the exact energy levels. Furthermore, it can be seen that the state assignments in terms of the pendular-state quantum numbers v_x, v_y, and m are appropriate to describe the energy levels. Note that the numerical calculations with the free-rotation basis set consider only m as a conserved quantity. While Eq. (26) properly reproduces the gross features of energy levels, some discrepancies appear in Fig. 2. These discrepancies originate from the neglect of the higher-order corrections. Their contribution becomes larger especially in the state-congested high v_x, v_y levels. Even in low v_x, v_y levels, discrepancies become apparent at high m levels. This is due to the neglect of Coriolis coupling as the second-order correction. The energy levels including the corrections perturbatively up to the second order are shown in Fig. 2(b). For example, the Coriolis coupling between the $(0,1)$ and $(1,0)$ states lowers the $(0,1)$ level down and lifts the $(1,0)$ level up as m increases. Similarly, the $(0,2)$ levels are pushed down and the $(1,1)$ levels are lifted up. These corrections provide better match up of the results by the present pendular formalism to the accurate calculations.

Because the energy-level representation of symmetric-top molecules in a strong-field limit has been reported previously [35], energy level comparison is not shown in this paper. Similar to the case of asymmetric tops, state assignments in terms of v, l, and m are very useful to discuss energy-level structures.

B. Spectra

Next we compare analytically derived spectra with simulations by the matrix diagonalization method using the free-rotation basis set. The size of basis set in the matrix diagonalization is set sufficiently large. Applying the theory described in Sec. II, basic structures and assignments of peaks in pendular-state spectra are discussed for several transition types classified in terms of the transition dipole operator, μ_{Fg}. Because our prime interest is on the evaluation of electronic transitions of large rigid molecules in a strong field, rotational constants of the initial and final states are fixed to be the same, and only λ changes in the following model calculations. It is assumed that μ directs to the b axis and that $\lambda'' = 0.055$, $\lambda' = 0.050$, $\sigma_x = 0.5$, $\sigma_y = 1.5$, and $\sigma_z = 1.0$, where double and single primes denote the ground and the excited states, respectively. The ground-state population is assumed as a Boltzmann distribution at $E_{\text{thermal}} = 30.0$. All the spectra presented herein are generated by the convolution of many lines with the linewidth of 0.1, for the sake of comparison of gross spectral features from different calculations.

As discussed in Sec. II E, there are six different types of excitation. For each of the three types of transitions, namely μ_z, μ_x, and μ_y types, two distinct configurations (parallel, μ_Z, and perpendicular, μ_X) exist. Since it is verbose to describe all types of spectra, we concentrate our discussion on the μ_{Zx} spectrum. The functional form of μ_{Zx} are presented in Eq. (37a). Considering the leading term of it, the gross spectrum feature comes from $(v_x' = v_x'' \pm 1, v_y' = v_y'', m' = m'')$ transitions. The matrix element of a transition dipole moment, $\langle \mu_{Zx} \rangle$, is approximated as shown in Eq. (38a). The corresponding transition energy, ΔE, up to the λ^0 order can be evaluated from Eqs. (25) and (26),

$$E = \Delta_0 \pm \frac{2\sigma_y^{1/2}}{\lambda'} + \left(\frac{1}{\lambda'} - \frac{1}{\lambda''}\right)[\sigma_y^{1/2}(2v_x'' + 1) + \sigma_x^{1/2}(2v_y'' + 1)] \mp \frac{\sigma_y}{4}\left(v_x'' + \frac{1}{2} \pm \frac{1}{2}\right) \pm \frac{1}{2}\left(\frac{4\sigma_z}{\sigma_x^{1/2}\sigma_y^{1/2}} - 3\sigma_x^{1/2}\sigma_y^{1/2}\right)\left(v_y'' + \frac{1}{2}\right), \tag{80}$$

where

$$\Delta_0 = -2[(\lambda')^{-2} - (\lambda'')^{-2}]. \tag{81}$$

Applying the above-mentioned model parameters, $\Delta_0 \approx -138.8$ and $2[(\lambda')^{-1} - (\lambda'')^{-1}] \approx 3.6$ are obtained. Corresponding spectrum is depicted in Fig. 3(a), and it is compared with the exact spectrum, Fig. 3(c). We can see that the exact spectrum is well predicted by the analytical representation, and the spectral features can be explained in terms of the pendular-state quantum numbers as follows: The series of

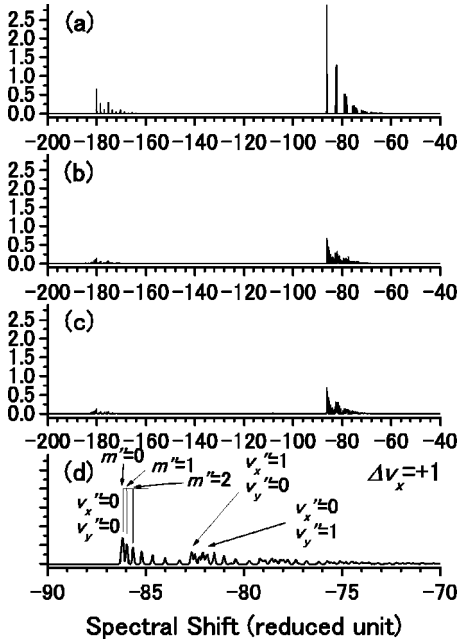

FIG. 3. Calculated spectra of an asymmetric top for a μ_{Zx} type transition from (a) the analytical representation, (b) the analytical representation with the second-order energy correction, and (c) the matrix diagonalization. (d) An expanded view of the $\Delta v_x=+1$, $\Delta v_y=0$ region in (c). The model parameters are described in the text.

lines started at −86 and −180 are $\Delta v_x=+1$ and $\Delta v_x=-1$ transitions, respectively, and their progressions are transitions with different $v''_{x,y}$ states. While the gross features are similar to one another, Fig. 3(a) fails to reproduce additional small splittings appearing in Fig. 3(c). This discrepancy comes from the Coriolis coupling. As discussed in Sec. IV A, the analytical energy representation of Eq. (26) does not contain the effect of Coriolis interaction, and the discrepancy in energy grows up as m increases. For example, the Coriolis interaction between the $(1,0)$ and $(0,1)$ levels lifts the $(1,0)$ level up as m increases, see Fig. 2(b). Thus, the $(1,0)\leftarrow(0,0)$ transitions shift to the blue side as m'' increases, and it results in a blue-shaded tail of the $(1,0)\leftarrow(0,0)$ transitions, as shown in Fig. 3(d). The red-shaded tail of the $\Delta v_x=-1$ transitions can be explained in the same way of the $\Delta v_x=+1$ transitions. This consideration is quantitatively verified by Fig. 3(b), which is calculated with the second-order correction to the energy and the analytical representation for transition oscillator strengths.

The other types of spectra can be well explained by a similar procedure, and the comparison of spectra is depicted in Figs. 4 and 5. In each type of transition, the analytical results well reproduce the exact spectra in the pendular state, and the all structures can be completely assigned in terms of the pendular-state quantum numbers, v_x, v_y, and m. We also carried out the same consideration for the case of symmetric-top molecules, and comfirmed that the pendular-limit formalism for symmetric tops, which is described in Sec. III, is very useful for prediction and explanation of spectra in the pendular state.

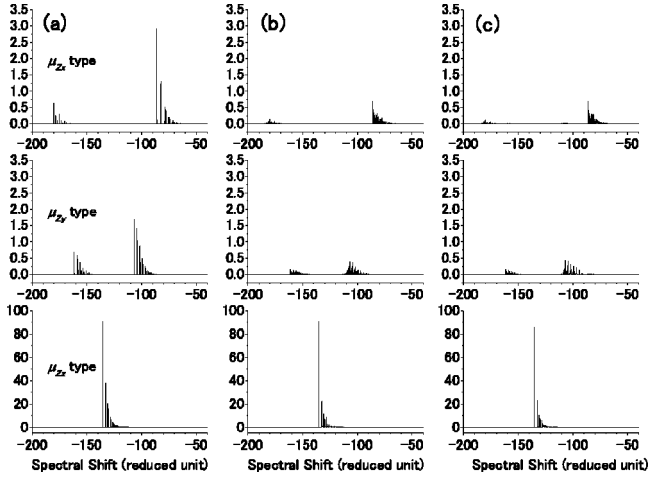

FIG. 4. Calculated spectra of an asymmetric top for μ_{Zg} type transitions $(g=x,y,z)$ from (a) the analytical representation, (b) the analytical representation with the second-order energy correction, and (c) the matrix diagonalization. The model parameters are the same as those used in Fig. 3.

V. CONCLUSION

Theoretical descriptions for the pendular-state spectroscopy of rigid symmetric- and asymmetric-top molecules have been reported in terms of a pendular-limit formalism. An energy-level representation of asymmetric-top molecules in the pendular limit has been derived analytically, and it has been found that the pendular states of asymmetric-top molecules are well described as two-dimensional anisotropic harmonic oscillator. Using the pendular-limit energy formulas and wave functions, selection rules and transition strengths for symmetric- and asymmetric-top molecules in a strong-field condition have been derived analytically. Throughout the theoretical considerations, we have used the symmetry groups for rigid bodies of symmetric- and asymmetric-tops in a uniform electric field, which have been

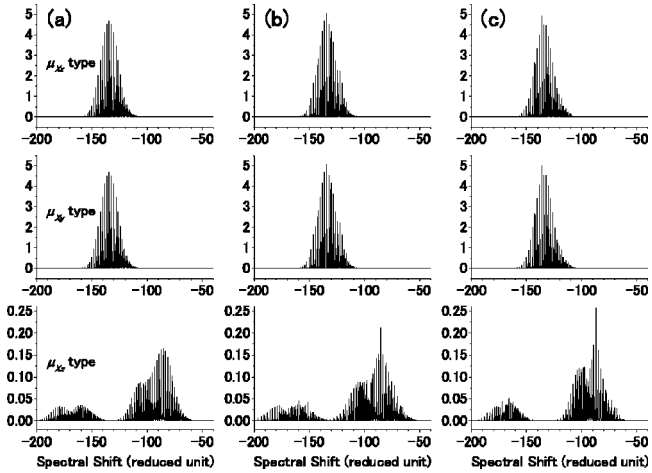

FIG. 5. Calculated spectra of an asymmetric top for μ_{Xg} type transitions $(g=x,y,z)$ from (a) the analytical representation, (b) the analytical representation with the second-order energy correction, and (c) the matrix diagonalization.

newly developed in this study. The utility of the analytical representations for energy levels and transition strengths is verified by comparing with the exact numerical calculations by matrix diagonalization.

ACKNOWLEDGMENTS

The authors thank Professor O. Kajimoto for his encouragement and support throughout the study. Valuable discussion with S. Kawai is also acknowledged. The present work has been partly supported by Grants-in-Aid (Nos. 14340180 and 15035206) from the Ministry of Education, Science, Culture, and Sports of Japan and the grants from the Japan Atomic Energy Research Institute, Sumitomo Science Foundation, and Photo Science and Technology Foundation.

APPENDIX A: PERTURBATION THEORY

Schrödinger equation is expressed as

$$\hat{H}\varphi_n - E_n\varphi_n = 0, \tag{A1}$$

where $\hat{H}$ is a full Hamiltonian, φ_n is an eigenfunction, and E_n is an eigenvalue. Then, $\hat{H}$, φ_n, and E_n are expanded as follows:

$$\hat{H} = \hat{H}^{(0)} + \hat{H}^{(1)} + \hat{H}^{(2)} + \cdots, \tag{A2a}$$

$$\varphi_n = \varphi_n^{(0)} + \varphi_n^{(1)} + \varphi_n^{(2)} + \cdots, \tag{A2b}$$

$$E_n = E_n^{(0)} + E_n^{(1)} + E_n^{(2)} + \cdots, \tag{A2c}$$

where the superscripts denote orders of perturbation, $\varphi_n^{(0)}$ is an eigenfunction of $\hat{H}^{(0)}$, and $E_n^{(0)}$ is eigenvalue of $\hat{H}^{(0)}$, namely,

$$\hat{H}^{(0)}\varphi_n^{(0)} = E_n^{(0)}\varphi_n^{(0)}, \tag{A3}$$

$\varphi_n^{(j)}$ is represented as

$$\varphi_n^{(j)} = \sum_i C_{ni}^{(j)}\varphi_i^{(0)}. \tag{A4}$$

Here, we regard the basis set of $\varphi_n^{(0)}$ not to be completely orthonormal but to be near orthonormal. $\hat{H}^{(n)}$ are not necessarily Hermite operators. If an exact volume element, $d\mathbf{v}$, is expanded as $d\mathbf{v}=(1+s^{(1)}+s^{(2)}+\cdots)d\mathbf{v}'$, where $d\mathbf{v}'$ is an approximated volume element with which integrals of $\varphi_n^{(0)}$ satisfy the orthonormal condition, overlap integrals are expanded as

$$\begin{aligned}\int \varphi_m^{(0)*}\varphi_n^{(0)}\, d\mathbf{v} &= \int \varphi_m^{(0)*}\varphi_n^{(0)}\, d\mathbf{v}' + \int \varphi_m^{(0)*}s^{(1)}\varphi_n^{(0)}\, d\mathbf{v}' \\ &\quad + \int \varphi_m^{(0)*}s^{(2)}\varphi_n^{(0)} d\mathbf{v}' + \cdots \\ &= \delta_{m,n} + S_{mn}^{(1)} + S_{mn}^{(2)} + \cdots,\end{aligned} \tag{A5}$$

where the superscripts also denote orders of perturbation. Matrix elements of $\hat{H}^{(j)}$ are represented by

$$\begin{aligned}\int \varphi_m^{(0)*}\hat{H}^{(j)}\varphi_n^{(0)}\, d\mathbf{v} &= \int \varphi_m^{(0)*}\hat{H}^{(j)}\varphi_n^{(0)} d\mathbf{v}' \\ &\quad + \int \varphi_m^{(0)*}s^{(1)}\hat{H}^{(j)}\varphi_n^{(0)} d\mathbf{v}' \\ &\quad + \int \varphi_m^{(0)*}s^{(2)}\hat{H}^{(j)}\varphi_n^{(0)} d\mathbf{v}' + \cdots \\ &= H_{mn}^{(j;0)} + H_{mn}^{(j;1)} + H_{mn}^{(j;2)} + \cdots,\end{aligned} \tag{A6}$$

where the perturbation order of $H_{mn}^{(j;k)}$ is $j+k$. From Eqs. (A5) and (A6), the following relation is obtained:

$$H_{mn}^{(j;k)} = \sum_i S_{mi}^{(k)} H_{in}^{(j;0)}. \tag{A7}$$

After the usual procedure of the normal perturbation theory, the first-order perturbation is represented as

$$E_n^{(1)} = H_{nn}^{(1;0)}, \tag{A8a}$$

$$C_{nm}^{(1)} = \frac{H_{mn}^{(1;0)}}{E_n^{(0)} - E_m^{(0)}} \quad (m \neq n), \tag{A8b}$$

$$C_{nn}^{(1)} = -\tfrac{1}{2}S_{nn}^{(1)}. \tag{A8c}$$

The second-order perturbation is expressed as

$$E_n^{(2)} = H_{nn}^{(2;0)} + \sum_k^{k\neq n} \frac{H_{nk}^{(1;0)}H_{kn}^{(1;0)}}{E_n^{(0)} - E_k^{(0)}}, \tag{A9a}$$

$$\begin{aligned}C_{nm}^{(2)} &= \sum_k^{k\neq n} \frac{H_{mk}^{(1;0)}H_{kn}^{(1;0)}}{(E_n^{(0)} - E_k^{(0)})(E_n^{(0)} - E_m^{(0)})} - \frac{H_{mn}^{(1;0)}H_{nn}^{(1;0)}}{(E_n^{(0)} - E_m^{(0)})^2} \\ &\quad + \frac{H_{mn}^{(2;0)} - \frac{1}{2}H_{mn}^{(1;0)}S_{nn}^{(1)}}{E_n^{(0)} - E_m^{(0)}} \quad (m \neq n),\end{aligned} \tag{A9b}$$

$$\begin{aligned}C_{nn}^{(2)} &= \frac{3}{8}(S_{nn}^{(1)})^2 - \frac{1}{2}S_{nn}^{(2)} - \sum_k^{k\neq n} \frac{\Re[S_{nk}^{(1)}H_{kn}^{(1;0)}]}{E_n^{(0)} - E_k^{(0)}} \\ &\quad - \frac{1}{2}\sum_k^{k\neq n} \frac{|H_{kn}^{(1;0)}|^2}{(E_n^{(0)} - E_k^{(0)})^2}.\end{aligned} \tag{A9c}$$

Therefore, $E_n^{(j)}$ and $C_{nm}^{(j)}$ are expressed with $H_{n'm'}^{(j';0)}$ and $S_{n'm'}^{(j')}$, both of which are matrix elements integrated with $d\mathbf{v}'$. The resultant energy-level representations are the same as the results of the normal perturbation theory.

APPENDIX B: FORMULAS OF SPECIAL FUNCTIONS

1. Hermite polynomials

The generating function of Hermite polynomials $H_n(\xi)$ is

$$e^{2t\xi - t^2} = \sum_{n=0}^{\infty} H_n(\xi)\frac{t^n}{n!}. \tag{B1}$$

If $\xi+\eta$ is substituted for ξ of Eq. (B1),

$$\sum_{n=0}^{\infty} H_n(\xi+\eta)\frac{t^n}{n!} = e^{2t\eta}e^{2t\xi-t^2} = \sum_{j=0}^{\infty}\sum_{k=0}^{\infty}(2\eta)^j H_k(\xi)\frac{t^{j+k}}{j!\,k!} = \sum_{s=0}^{\infty}\left[\sum_{k=0}^{s}(2\eta)^{s-k}H_k(\xi)\frac{s!}{k!\,(s-k)!}\right]\frac{t^s}{s!} \tag{B2}$$

is yielded. Then,

$$H_n(\xi+\eta) = \sum_{k=0}^{n}\frac{n}{k!\,(n-k)!}(2\eta)^{n-k}H_k(\xi) \tag{B3}$$

is obtained. Therefore,

$$H_n(a\xi) = \sum_{k=0}^{n}\frac{n}{k!\,(n-k)!}[2(a-1)\xi]^{n-k}H_k(\xi) \tag{B4}$$

can be derived.

2. Associated Laguerre polynomials

The generating function of associated Laguerre polynomials $L_n^{\alpha}(\xi)$ is

$$\frac{(-t)^{\alpha}e^{-t\xi/(1-t)}}{(1-t)^{\alpha+1}} = \sum_{n=\alpha}^{\infty}L_n^{\alpha}(\xi)\frac{t^n}{n!}. \tag{B5}$$

By the substitution of $\xi+\eta$ for ξ,

$$\sum_{n=\alpha}^{\infty}L_n^{\alpha}(\xi+\eta)\frac{t^n}{n!} = \frac{(-t)^{\alpha}e^{-t\xi/(1-t)}}{(1-t)^{\alpha+1}}e^{-t\eta/(1-t)} = \sum_{j=0}^{\infty}\frac{\eta^j}{j!}\frac{(-t)^{\alpha+j}e^{-t\xi/(1-t)}}{(1-t)^{\alpha+j+1}} = \sum_{j=0}^{\infty}\sum_{k=\alpha+j}^{\infty}\frac{\eta^j}{j!}L_k^{\alpha+j}(\xi)\frac{t^k}{k!} = \sum_{k=\alpha}^{\infty}\left[\sum_{j=0}^{k-\alpha}\frac{\eta^j}{j!}L_k^{\alpha+j}(\xi)\right]\frac{t^k}{k!}. \tag{B6}$$

Thus, Eq. (B7) is derived,

$$L_n^{\alpha}(\xi+\eta) = \sum_{k=0}^{n-\alpha}\frac{\eta^k}{k!}L_n^{\alpha+k}(\xi). \tag{B7}$$

Then,

$$L_n^{\alpha}(a\xi) = \sum_{k=0}^{n-\alpha}\frac{[(a-1)\xi]^k}{k!}L_n^{\alpha+k}(\xi). \tag{B8}$$

[1] H. J. Loesch and A. Remscheid, J. Chem. Phys. **93**, 4779 (1990).
[2] B. Friedrich and D. R. Herschbach, Z. Phys. D: At., Mol. Clusters **18**, 153 (1991).
[3] P. A. Block, E. J. Bohac, and R. E. Miller, Phys. Rev. Lett. **68**, 1303 (1992).
[4] H. J. Loesch and A. Remscheid, J. Phys. Chem. **95**, 8194 (1991).
[5] B. Friedrich and D. Herschbach, J. Chem. Phys. **111**, 6157 (1999).
[6] B. Friedrich and D. Herschbach, Phys. Chem. Chem. Phys. **2**, 419 (2000).
[7] B. Friedrich, D. P. Pullman, and D. R. Herschbach, J. Phys. Chem. **95**, 8118 (1991).
[8] B. Friedrich, D. R. Herschbach, J. M. Rost, H. G. Rubahn, M. Renger, and M. Verbeek, J. Chem. Soc., Faraday Trans. **89**, 1539 (1993).
[9] K. J. Franks, H. Li, and W. Kong, J. Chem. Phys. **110**, 11779 (1999).
[10] H. Li, K. J. Franks, R. J. Hanson, and W. Kong, J. Phys. Chem. A **102**, 8084 (1998).
[11] W. Kong and J. Bulthuis, J. Phys. Chem. A **104**, 1055 (2000).
[12] A. Durand, J. C. Loison, and J. Vigué, J. Chem. Phys. **106**, 477 (1997).
[13] A. Durand, J. C. Loison, and J. Vigué, J. Chem. Phys. **101**, 3514 (1994).
[14] A. Slenczka, B. Friedrich, and D. Herschbach, Chem. Phys. Lett. **224**, 238 (1994).
[15] R. Kanya and Y. Ohshima, Chem. Phys. Lett. **370**, 211 (2003).
[16] K. J. Castle, J. Abbott, X. Peng, and W. Kong, J. Chem. Phys. **113**, 1415 (2000).
[17] K. J. Castle and W. Kong, J. Chem. Phys. **112**, 10156 (2000).
[18] K. Nauta and R. E. Miller, J. Chem. Phys. **117**, 4846 (2002).
[19] K. Nauta and R. E. Miller, Phys. Rev. Lett. **82**, 4480 (1999).
[20] K. Nauta and R. E. Miller, J. Chem. Phys. **111**, 3426 (1999).
[21] K. Nauta and R. E. Miller, Science **283**, 1895 (1999).
[22] K. Nauta and R. E. Miller, J. Chem. Phys. **111**, 3426 (1999).
[23] K. Nauta, D. T. Moore, and R. E. Miller, Faraday Discuss. **113**, 261 (1999).
[24] L. Oudejans and R. E. Miller, J. Phys. Chem. **99**, 13670 (1995).
[25] L. Oudejans and R. E. Miller, J. Chem. Phys. **109**, 3474 (1994).
[26] L. Oudejans and R. E. Miller, J. Phys. Chem. A **101**, 7582 (1997).
[27] G. Bazalgette, R. White, G. Trénec, E. Audouard, M. Büchner, and J. Vigué, J. Phys. Chem. A **102**, 1098 (1998).
[28] K. J. Castle, J. E. Abbott, X. Peng, and W. Kong, J. Phys. Chem. A **104**, 10419 (2000).
[29] F. Brouwer, Ph.D. thesis, Univ. Utrecht, 1930.
[30] H. K. Hughes, Phys. Rev. **72**, 614 (1947).
[31] C. Schlier, Z. Phys. **141**, 16 (1955).
[32] M. Peter and M. W. Strandberg, J. Chem. Phys. **26**, 1657 (1957).

[33] K. von Meyenn, Z. Phys. **231**, 154 (1970).
[34] J. Bulthuis, J. van Leuken, F. van Amerom, and S. Stolte, Chem. Phys. Lett. **222**, 378 (1994).
[35] A. I. Maergoiz and J. Troe, J. Chem. Phys. **99**, 3218 (1993).
[36] J. M. Rost, J. C. Griffin, B. Friedrich, and D. R. Herschbach, Phys. Rev. Lett. **68**, 1299 (1992).
[37] D. T. Moore, L. Oudejans, and R. E. Miller, J. Chem. Phys. **110**, 197 (1999).
[38] J. K. G. Watson, Can. J. Phys. **53**, 2210 (1975).